

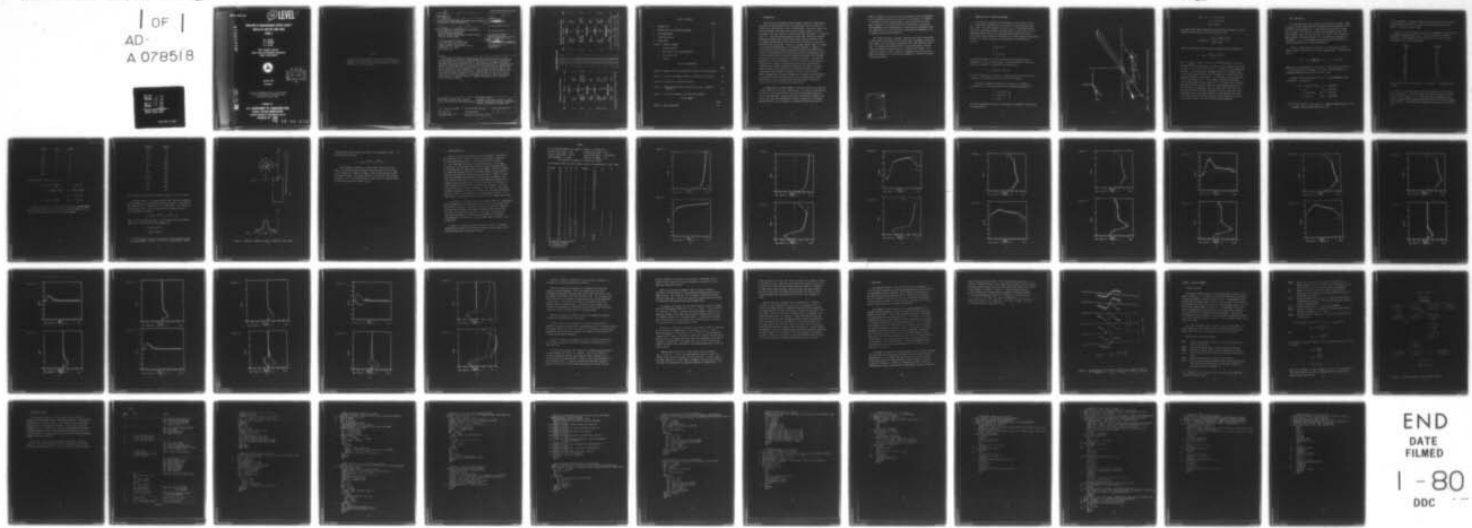
AD-A078 518 NATIONAL OCEANIC AND ATMOSPHERIC ADMINISTRATION BOUL--ETC F/G 17/9  
SIMULATION OF RADAR-MEASURED DOPPLER VELOCITY PROFILES IN LOW-L--ETC(U)  
FEB 78 W B SWEZY , W R MONINGER DOT-FA76WAI-622

UNCLASSIFIED

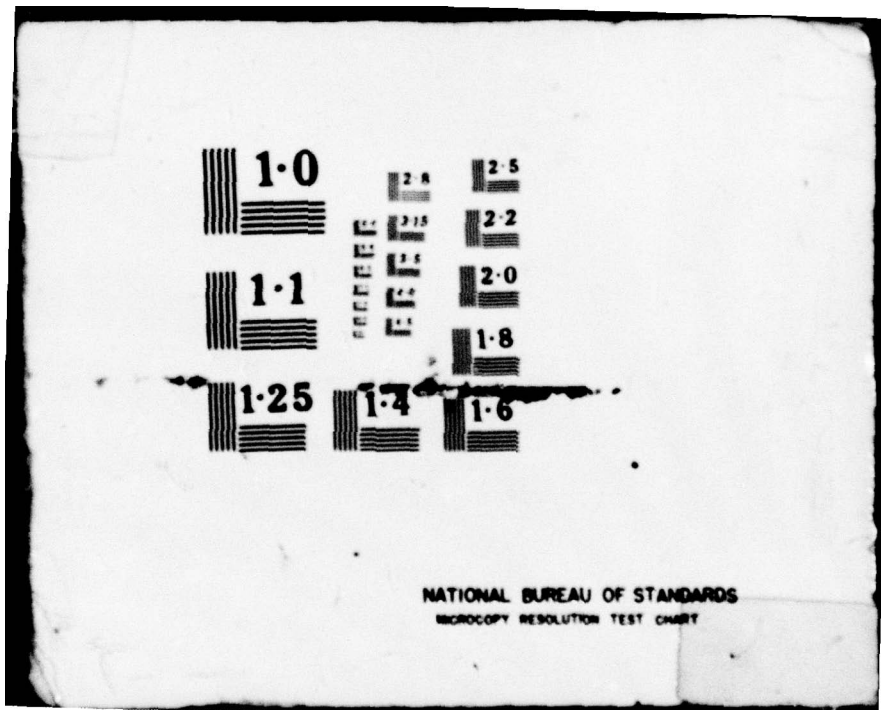
OF  
AD-  
A 078518

FAA-RD-78-46

NL



END  
DATE  
FILED  
I - 80  
DDC



12

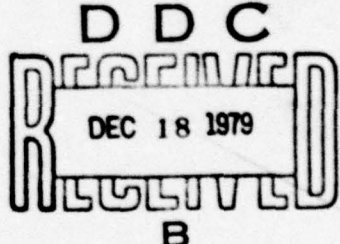
LEVEL II

ADA 078518

SIMULATION OF RADAR-MEASURED DOPPLER VELOCITY  
PROFILES IN LOW-LEVEL WIND SHEAR  
(PHASE I)

W. B. Sweeny  
W. R. Meninger  
R. G. Strauch

Wave Propagation Laboratory  
National Oceanic and Atmospheric Administration  
Boulder, Colorado 80302



February 1978  
Final Report

DOC FILE COPY  
DOC

Document is available to the U.S. public through  
the National Technical Information Service,  
Springfield, Virginia 22161.

Prepared for  
U.S. DEPARTMENT OF TRANSPORTATION  
FEDERAL AVIATION ADMINISTRATION  
Systems Research & Development Service  
Washington, D.C. 20590

79 12 10 013

NOTICE

This document is disseminated under the sponsorship of the Department of Transportation in the interest of information exchange. The United States Government assumes no liability for its contents or use thereof.

## Technical Report Documentation Page

1. Report No. FAA-RD-78-46	2. Government Accession No.	3. Recipient's Catalog No. 12531	
4. Title and Subtitle SIMULATION OF RADAR-MEASURED DOPPLER VELOCITY PROFILES IN LOW-LEVEL WIND SHEAR. (PHASE I).			
5. Report Date February 1978			
6. Performing Organization Code			
7. Author(s) W. B. Sweezy, W. R. Moninger R. G. Strauch			
8. Performing Organization Report No.			
9. Performing Organization Name and Address Wave Propagation Laboratory National Oceanic and Atmospheric Administration, Boulder, Colorado 80302			
10. Work Unit No. (TRAILS)			
11. Contract or Grant No. DOT-FA76 WAI-622 IAA-Task VII			
12. Sponsoring Agency Name and Address U.S. Department of Transportation Federal Aviation Administration Systems Research & Development Service Washington, D.C. 20590			
13. Type of Report and Period Covered Final Report January 1977 to August 1977			
14. Sponsoring Agency Code FAA/ARD-243			
15. Supplementary Notes			
16. Abstract A computer simulation of radar-measured radial velocity profiles was made to evaluate the effects of finite antenna beamwidth and the location of the radar on the measurement of low-level wind shear. The inputs to the computer simulation program are the radar characteristics and the existing wind field - the outputs are the wind component along any line (usually the glide path) and the radar-measured radial velocity profile for a given antenna location and antenna pointing. The results show that a radar beamwidth of 1.5 deg. provides sufficient spatial resolution to measure low-level wind profiles. However, when the wind fields contain horizontal gradients, headwinds and tailwinds encountered by an aircraft on the glide path cannot be measured by a fixed-beam radar that is offset from the end of the runway. A steerable antenna is needed to adequately measure the wind profile for these cases.			
17. Key Words Wind shear, Doppler radar, Aircraft safety, Wind profiles, and Severe weather	18. Distribution Statement Document is available to the U.S. public through the National Technical Information Service, Springfield, Virginia 22161		
19. Security Classif. (of this report) Unclassified	20. Security Classif. (of this page) Unclassified	21. No. of Pages 48	22. Price

406 292

METRIC CONVERSION FACTORS

Approximate Conversions from Metric Measures									
Symbol	What You Know	Multiply by	To Find						
LENGTH									
inches	12.5	centimeters	feet	0.034	centimeters	inches	centimeters	feet	yards
feet	30	centimeters	yards	0.4	centimeters	feet	centimeters	feet	yards
yards	9.3	centimeters	kilometers	2.3	centimeters	feet	centimeters	feet	yards
miles	1.6	centimeters	kilometers	1.1	centimeters	feet	centimeters	feet	yards
AREA									
square inches	6.5	square centimeters	square feet	0.14	square centimeters	square inches	square centimeters	square feet	square yards
square feet	0.039	square centimeters	square kilometers	1.2	square centimeters	square feet	square centimeters	square feet	square yards
square yards	0.8	square centimeters	hectares	0.4	square centimeters	square feet	square centimeters	square feet	square yards
square miles	2.6	square centimeters	hectares (10,000 m <sup>2</sup> )	2.5	square centimeters	square kilometers	square centimeters	square kilometers	square miles
MASS (weight)									
grams	20	grams	ounces	0.035	grams	ounces	grams	ounces	ounces
ounces	0.46	grams	grams	2.2	grams	ounces	ounces	ounces	ounces
pounds	0.9	grams	grams	1.1	grams	ounces	ounces	ounces	ounces
VOLUME									
milliliters	1	milliliters	milliliters	0.03	milliliters	fluid ounces	milliliters	fluid ounces	fluid ounces
liters	15	milliliters	liters	2.1	milliliters	fluid ounces	milliliters	fluid ounces	fluid ounces
fluid ounces	30	milliliters	liters	1.06	milliliters	fluid ounces	milliliters	fluid ounces	fluid ounces
cups	0.24	liters	liters	0.26	liters	gallons	liters	gallons	gallons
pints	0.47	liters	liters	2.6	liters	cubic feet	liters	cubic feet	cubic yards
quarts	0.95	liters	liters	1.3	liters	cubic meters	liters	cubic meters	cubic yards
gallons	2.0	liters	cubic meters	0.76	cubic meters	cubic yards	cubic meters	cubic yards	cubic yards
TEMPERATURE (heat)									
degrees Celsius	5.0	degrees Celsius	degrees Celsius	9.1 (50° Fahrenheit)	degrees Celsius	degrees Fahrenheit	degrees Celsius	degrees Fahrenheit	degrees Fahrenheit
degrees Fahrenheit	9.0	degrees Celsius	degrees Celsius	50 (9.1° Celsius)	degrees Celsius	degrees Fahrenheit	degrees Celsius	degrees Fahrenheit	degrees Fahrenheit

UNIVERSITY OF TORONTO LIBRARIES  
UNIVERSITY OF TORONTO LIBRARY COLLECTIONS ARE HELD UNDER THE  
CUSTODY OF THE UNIVERSITY OF TORONTO LIBRARIES, 149  
UNIVERSITY AVENUE, TORONTO, ONTARIO, CANADA M5S 1J4.  
TEL: 416-978-3434 FAX: 416-978-3435 E-MAIL: [LIBRARY@UTORONTO.CA](mailto:LIBRARY@UTORONTO.CA)

## TABLE OF CONTENTS

	Page
1. INTRODUCTION	1
2. FORMULATION OF THE SIMULATION PROGRAM	3
3. WIND SHEAR MODELS	6
4. SIMULATION RESULTS	12
5. CONCLUSIONS	30
APPENDIX: COMPUTER PROGRAM	33
1. Program Structure	33
2. Description of the Program Modules	33
3. Data Input-Output	36
4. Listing	37

## LIST OF ILLUSTRATIONS

	Page
Figure 2.1 Radar location and orientation relative to the glide path.	4
Figure 3.1 Location of downburst (model 6) relative to the runway.	10
Figures 4.1 through 4.26 Simulation results.	14
Figure 5.1 Radar-measured radial velocity profiles for a downburst (model 6).	32
Figure A.1 Structure diagram for the simulation program.	35

## LIST OF TABLES

	Page
TABLE A.1 Data Input-Output	37

## 1. INTRODUCTION

Over the past few decades microwave Doppler radars have demonstrated the ability to measure wind fields in regions where there is sufficient reflectivity from particles, such as precipitation, to provide a radar echo. Recent experiments have shown that sensitive Doppler radars can detect and measure the radial velocity of refractive-index fluctuations in optically clear air. Using the Velocity-Azimuth Display (VAD) technique, Frequency Modulated-Continuous Wave (FM-CW) Doppler radar and pulse Doppler radar can measure average wind profiles from either precipitation scatterers or refractive-index scattering. Therefore, microwave Doppler radar is capable of providing wind measurements in all weather conditions. However, a vertical profile of the average horizontal wind near a particular point, such as the touchdown point or middle marker, may not be adequate to warn aircraft of the presence of dangerous winds during take-off and landing when the wind field is spatially or temporally variable. The radar must be capable of accurately measuring the radial velocity at low elevation angles and short ranges to determine the wind profile encountered by aircraft on the landing and take-off paths near the runway. An experimental program is being conducted at the National Aviation Facilities Experimental Center (NAFEC) to determine if an air traffic control radar, equipped with a suitable antenna and with Doppler data processing, has sufficient sensitivity and resolution to accurately measure radial wind profiles at low elevation angles and short ranges in optically clear air (as well as in regions of precipitation).

The mean Doppler velocity depends on the radial velocity distribution of the scatterers in the radar resolution cell, so that the radar-measured velocity is a filtered version of the actual wind component along the axis of the radar beam. Velocity gradients existing over distances much smaller than the radar beamwidth will cause a broadening of the Doppler spectrum but will not be revealed by the radar-measured mean velocity.

Velocity gradients existing over distances comparable with the beamwidth will be smoothed so that peak values will not be detected. Furthermore, if the radar is offset from the runway so that the axis of the radar beam is parallel to but displaced from the flight path, the measured wind component will be representative of the actual wind component along the flight path only if the wind field is horizontally homogeneous (i.e., if there are no horizontal gradients).

This report describes a computer simulation for testing the effects of both finite radar resolution volume and radar displacement relative to the runway on the radar-measured component of the wind along the flight path. The simulation program contains six wind shear models, and the results obtained with these models are included in this report. The simulation program is general enough to accommodate any analytical wind model that expresses the Cartesian wind components in terms of Cartesian position coordinates.

ACCESSION for	
NTIS	White Section <input checked="" type="checkbox"/>
One	Buff Section <input type="checkbox"/>
UNCLASSIFIED	
NS 100-100	
BY	
DECLASSIFICATION DATES	
SPECIAL	
A	

## 2. FORMULATION OF THE SIMULATION PROGRAM

The location of the radar and the runway are illustrated in Figure 2.1. The nominal touchdown point is the origin of the Cartesian coordinate system. The radar location is at  $(X_R, Y_R, 0)$ . The azimuth pointing angle (AZ) is measured clockwise from the positive y direction, and the elevation pointing angle (EL) is measured upward from the horizontal. The aircraft travels along the glide path at an angle  $\phi_G$  from the horizontal, so that, at a radial distance  $R_G$  from touchdown, its coordinates are given by

$$x = R_G \cos \phi_G$$

$$y = 0$$

$$z = R_G \sin \phi_G.$$

The analytical models of the wind field provide the Cartesian wind components  $u$ ,  $v$ , and  $w$  for any  $(x, y, z)$ . The wind component in the direction of the aircrafts' flight path is calculated from

$$V_G = u \cos \phi_G + w \sin \phi_G.$$

With this formulation, a tailwind is a negative glide-slope velocity and a headwind is a positive velocity for an aircraft landing.

A spherical coordinate system with its origin at the radar has coordinates  $(r, \theta, \phi)$  that are related to the Cartesian coordinates by

$$x = r \sin \theta \cos \phi + X_R$$

$$y = r \cos \theta \cos \phi + Y_R$$

$$z = r \sin \phi.$$

The radial component of the wind, at any point, is related to the Cartesian wind components by

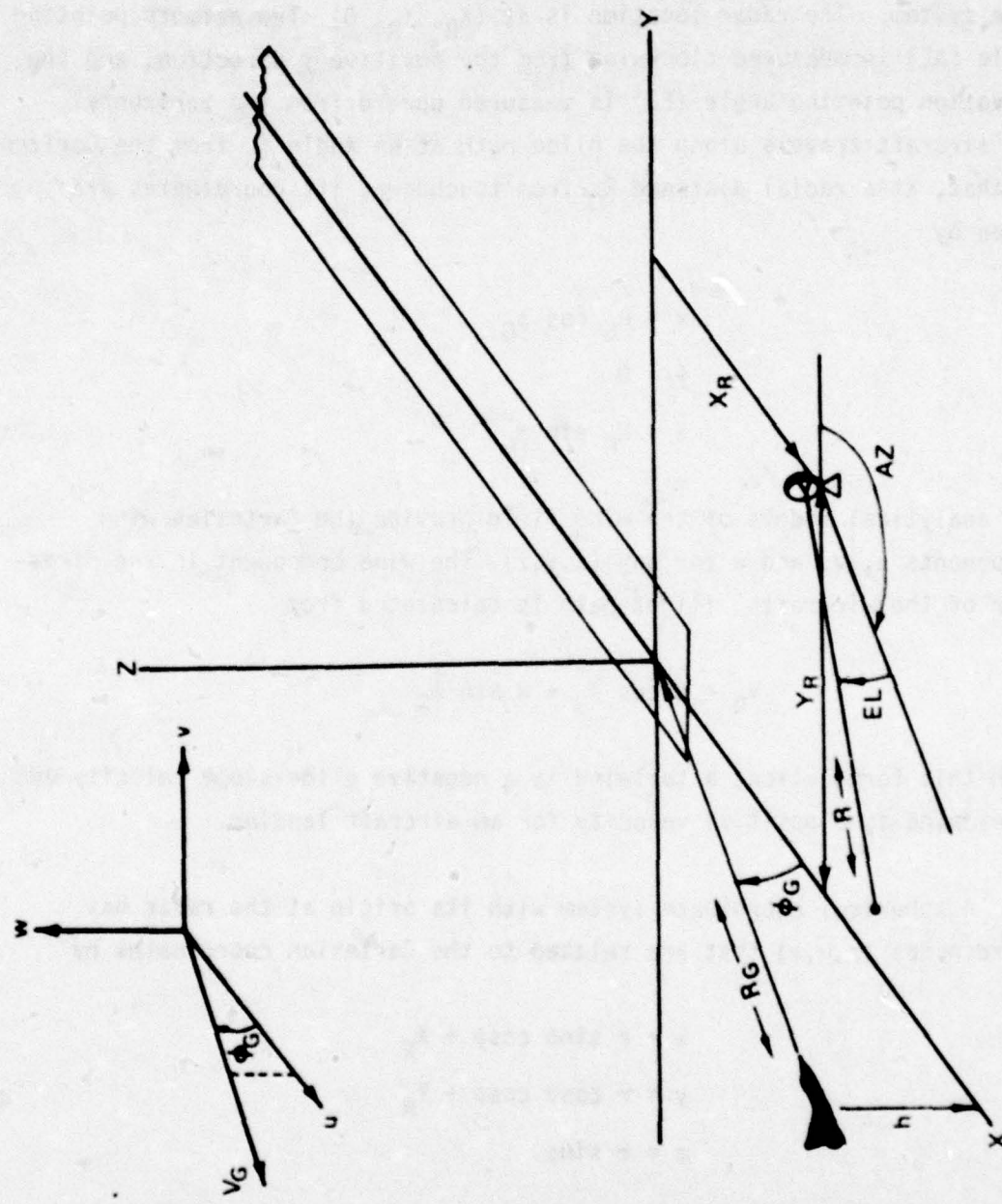


Figure 2.1 Radar location and orientation relative to the glide path.

$$\begin{aligned}
 V_R(r, \theta, \phi) = & u(r, \theta, \phi) \sin \theta \cos \phi \\
 & + v(r, \theta, \phi) \cos \theta \cos \phi \\
 & + w(r, \theta, \phi) \sin \phi.
 \end{aligned}$$

We assume uniform radar reflectivity and calculate the theoretical radar-measured radial velocity at the point (R, AZ, EL) from

$$V_M(R, AZ, EL) = \frac{\int V_R(r, \theta, \phi) W(r, \theta, \phi) dV}{\int W(r, \theta, \phi) dV},$$

where  $W$  is the two-way radar antenna illumination function defined by

$$W = \exp \left[ \frac{-(\theta - AZ)^2 - (\phi - EL)^2}{2\Delta^2} \right],$$

and  $\Delta = \frac{B}{\sqrt{8 \ln 4}}$ , where  $B$  is the 1-way antenna beamwidth. The volume element  $dV = (dr)(rd\phi)(rcos\phi d\theta)$ . The limits of the integration are taken as  $|r-R| \leq ct/4$ ,  $|\theta - AZ| \leq m\Delta$ , and  $|\phi - EL| \leq m\Delta$  where  $\tau$  is the radar pulse duration,  $c$  is the velocity of propagation and  $m$  is a constant (equal to 3.1) which assures that the error introduced by ignoring part of the antenna illumination is negligible. The integration extends beyond the -20 dB illumination points. The integral is evaluated numerically, using volume elements of the order of  $10^{-3} m^3$ . The actual wind component along the glide path and the theoretical radar-measured radial velocity are displayed for comparison. The calculated radial velocities are expected values that would be measured by an actual radar with random measurement error. The radar resolution volume low-pass filters the true radial wind field so the resolution of the measured wind depends on the pulse length of the radar and the antenna beamwidth.

### 3. WIND SHEAR MODELS

Six wind shear models were included in the simulation program. Models 1 through 5 do not contain horizontal gradients and are therefore vertical profiles of the horizontal wind. These profiles are the same at every (x,y) location. The first four profiles were developed by Fichtl and Camp<sup>1</sup> of NASA's Space Sciences Laboratory for the FAA. The fifth profile was presented in a memo by Langweil<sup>2</sup>. The sixth model was developed by the authors. It is a three-dimensional wind model with horizontal and vertical gradients of all three wind components.

Profile 1 (Fichtl and Camp's profile 1) is a logarithmic profile that is typical of the wind in the neutral boundary layer. The functional form is

$$V(Z) = V(20) \left[ \frac{\ln(Z/1.5)}{\ln(13.33)} \right] \text{ for } 1.5 \leq Z \leq 1500 \text{ feet,}$$

where  $V(Z)$  is the magnitude of the horizontal wind at height  $Z$  and  $V(20)$  is the reference level wind taken as 11.5 m/s. The wind direction is constant with height and the vertical wind is zero.

Profile 2 (Fichtl and Camp's profile 3) is the recommended frontal wind profile. The profile is

$$\begin{aligned} V(Z) &= 3.5(Z/20)^{0.43} \text{ (m/s)} & 0 \leq Z \leq 1500 \text{ feet} \\ \theta &= \theta_0 & 0 \leq Z \leq 100 \text{ feet} \\ \theta &= 0.4(Z-100) + \theta_0 & 100 \leq Z \leq 400 \text{ feet} \\ \theta &= 120 + \theta_0 & 400 \leq Z \leq 1500 \text{ feet.} \end{aligned}$$

<sup>1</sup> G. H. Fichtl and D. W. Camp, letter to F. Melewicz dated January 23, 1976.

<sup>2</sup> L. Langweil, FAA memo dated February 17, 1976.

$\theta$  is the direction (in degrees) toward which the wind is blowing, measured counterclockwise from the x-axis, and  $\theta_0$  is the wind direction at the surface. The vertical wind is zero.

Profile 3 (Fichtl and Camp's profile 2) is recommended for representing the nighttime stable boundary layer. The wind direction is constant with height. The magnitude of the horizontal wind is given by a linear interpolation from the following table.

<u>Z(feet)</u>	<u>V(knots)</u>
30	2.7
75	4.1
150	6.9
300	8.3
450	11.4
600	10.5
750	9.2
900	8.2
1050	8.0
1200	7.9
1300	7.8
1500	7.8

Below 30 feet the wind is given by  $V = 2.7 (Z/30)^{.45}$ . The vertical wind is zero.

Profile 4 (Fichtl and Camp's profile 4) represents cold air outflow from a thunderstorm. The profile shows the winds encountered by the aircraft at various heights. It is a one-dimensional representation that does not include the horizontal gradients that would be found with thunderstorm outflows. The horizontal wind components are given in the following table.

<u>Z(feet)</u>	<u>u(knots)</u>	<u>v(knots)</u>
0	-10	3
20	-10	3
200	-5	8
300	+15	8
450	+30	10
750	+7	13
1500	+7	10

The vertical wind in ft/sec is given by

$$w = (-5.04) \sin\left(\frac{\pi(330-Z)}{140}\right), \quad 50 \leq Z \leq 330 \text{ feet}$$

$$= (10.13)\left(\frac{460-Z}{130}\right)\left[\left(\frac{460-Z}{130}\right)^2 - 1\right] + 22.11\left(\frac{460-Z}{130}\right)\left(\frac{590-Z}{130}\right),$$

$$330 \leq Z \leq 460 \text{ feet}$$

$$w = -16.94 \sin\left[\frac{\pi(770-Z)}{320}\right] \quad 460 \leq Z \leq 770 \text{ feet}.$$

Profile 5 (Langweil), an alternative to profile 3, has been shown to be more difficult for pilots to handle in flight trainers. It is given by linear interpolation from the following table.

<u>V(knots)</u>	<u>Z(feet)</u>
7.7	30
11.6	75
19.6	150
23.7	300
32.4	450
30	600
26.2	750
24.6	900
22.9	1050
22.6	1200
22.3	1300
22.3	1500

Wind direction is constant with height and there is no vertical wind.

Wind shear model 6 is an analytic model that simulates a downburst from a thunderstorm as depicted by Fujita and Caracena<sup>3</sup>. The center of the downburst ( $X_C, Y_C$ ) (see Figure 3.1) is adjustable. The direction of the horizontal wind is radially outward from the downburst center, and the magnitude is given by

$$V_R = 150Z e^{-(10Z)^2} \frac{1}{R} (1-e^{-(2R)^2}) \text{ m/s,}$$

where  $Z$  is the altitude (km) and  $R$  is the distance from the downburst center (km). The horizontal wind components are

$$u = V_R (X - X_C) / R \text{ m/s}$$

$$v = V_R (Y - Y_C) / R \text{ m/s.}$$

---

<sup>3</sup> T. T. Fujita and F. Caracena, "An analysis of three weather-related aircraft accidents", in *Bull. Am. Met. Soc.*, 58, 1977, pp. 910-918.

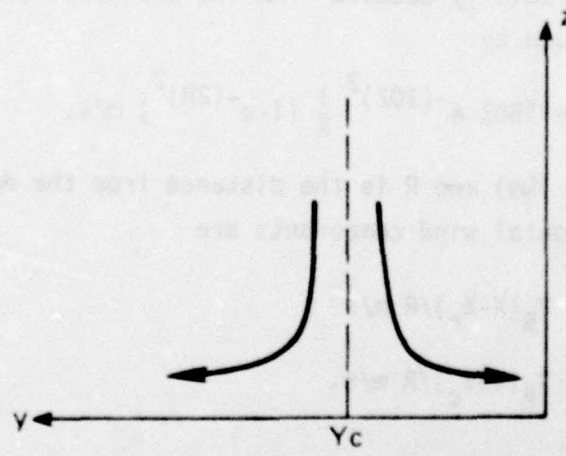
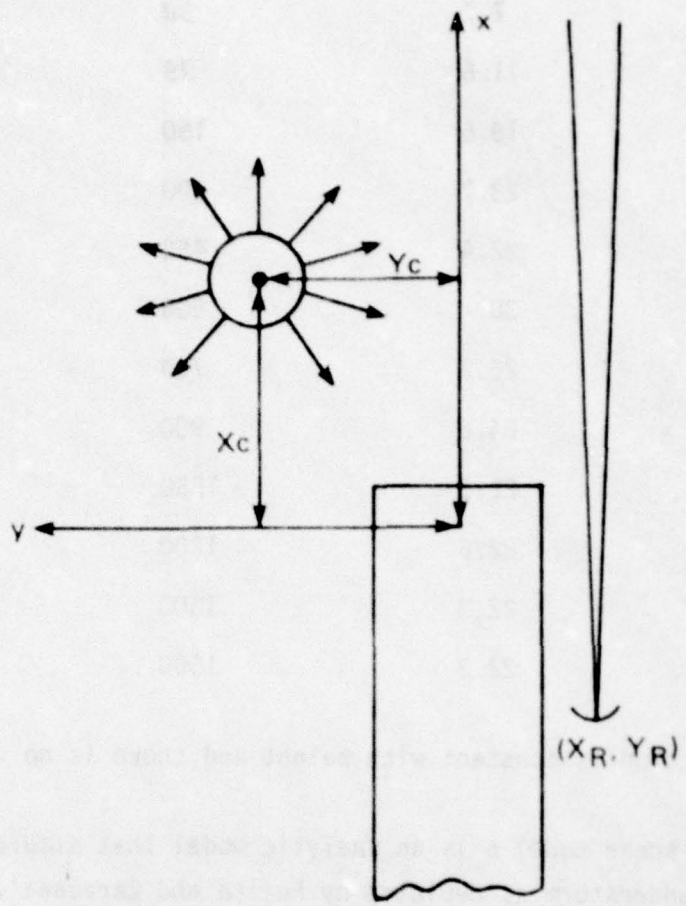


**Figure 3.1** Location of downburst (model 6) relative to the runway.

The maximum horizontal winds occur 560 m from the downburst center. The vertical wind is given by

$$w = -6(1-e^{-(10z)^2}) e^{-(2R)^2} \text{ m/s.}$$

In the computer simulations a minimum radar range of 450 m was used. This minimum range was chosen so that the location of the radar could be taken as 0 m above the runway without having negative heights in the pulse volume. The minimum height for calculating radar measured winds was 23.5 m. The minimum range of actual radars is expected to be at least 450 m because of ground clutter.

#### 4. SIMULATION RESULTS

Profiles 1-5 have no horizontal position dependence; consequently, the offset position of the radar relative to the runway is immaterial for wind speed-height profiles. The wind direction for profiles 1, 3, and 5 was made constant with height and parallel to the runway. For profile 2, the wind direction varied with height and the direction at the ground was also taken parallel to the runway. Figure 4.1 through 4.15 show the simulation results, with three figures for each profile. The actual wind profile encountered by the aircraft is shown as a solid line; the simulated radar-measured points are shown as diamonds. The first figure in each group of three is a wind speed-height profile for a 3-degree antenna elevation angle, and the third figure in the group is a wind speed-height profile for a 6-degree elevation angle. Since the offset position of the radar is immaterial, it was taken as zero (radar located at touchdown). Therefore, the radar range and the distance along the glide slope are the same only for a 3-degree elevation angle. The second figure in each group shows the winds along the 3-degree glide slope.

In all cases, the minimum range of the radar was 450 m (3 microseconds), which corresponds to a minimum altitude of 23 m for a 3-degree elevation. For profiles 2 through 5, the input wind profile extends to a 1500-foot altitude; above 1500 feet, the computer program set the wind to zero. This causes an unrealistic wind shear in the input, but it serves to illustrate the problem of finite antenna beamwidth at long range as discussed below. For profile 1, the input model does not return to zero at 1500 feet.

Figures 4.1 through 4.26 present simulation results. The legend appearing below contains the information common to every figure and the variables specifically appropriate to each.

Legend

The following parameters are common to Figures 4.1 through 4.26.

Aircraft glide slope - 3 deg	Minimum radar range - 450 m
Runway azimuth angle - 90 deg	Radar pulse length - 1 microsecond
Radar beamwidth - 1.5 deg	Sampling increments - 10 m

All plotted wind speeds are in meters per second

The following table lists the variables specifically appropriate to each figure.

<u>FIG. NO.</u>	<u>AZ</u>	<u>EL</u>	<u>XR</u>	<u>YR</u>	<u>Profile</u>	<u><math>\theta</math></u>	<u>XC</u>	<u>YC</u>
4.1	90	3	0	0	1	90	-	-
4.2	90	3	0	0	1	90	-	-
4.3	90	6	0	0	1	90	-	-
4.4	90	3	0	0	2	90*	-	-
4.5	90	3	0	0	2	90*	-	-
4.6	90	6	0	0	2	90*	-	-
4.7	90	3	0	0	3	90	-	-
4.8	90	3	0	0	3	90	-	-
4.9	90	6	0	0	3	90	-	-
4.10	90	3	0	0	4	90	-	-
4.11	90	3	0	0	4	90	-	-
4.12	90	6	0	0	4	90	-	-
4.13	90	3	0	0	5	90	-	-
4.14	90	3	0	0	5	90	-	-
4.15	90	6	0	0	5	90	-	-
4.16	90	3	0	0	6	-	.5	.5
4.17	90	3	0	0	6	-	.5	.5
4.18	90	6	0	0	6	-	.5	.5
4.19	90	3	-0.1	-0.1	6	-	.5	.5
4.20	90	3	-0.1	-0.1	6	-	.5	.5
4.21	90	6	-0.1	-0.1	6	-	.5	.5
4.22	90	3	-2.5	0.1	6	-	.5	0
4.23	90	3	-2.5	0.1	6	-	.5	0
4.24	90	6	-2.5	0.1	6	-	.5	0
4.25	60	3	0	0	2	90*	-	-
4.26	120	3	0	0	2	90*	-	-

\* Wind direction at the ground.

All angles in degrees

All distances in km

$\theta$  = wind direction

Figure 4.1

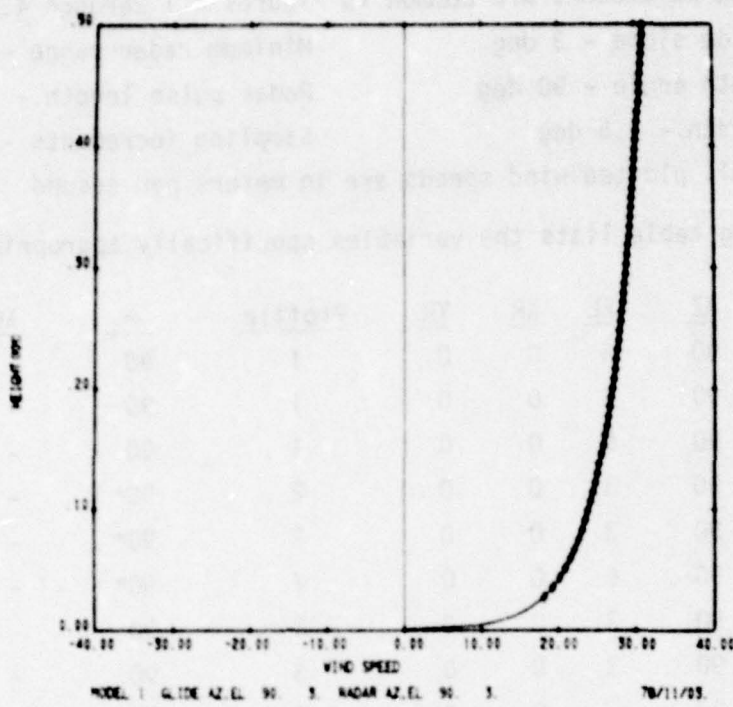


Figure 4.2

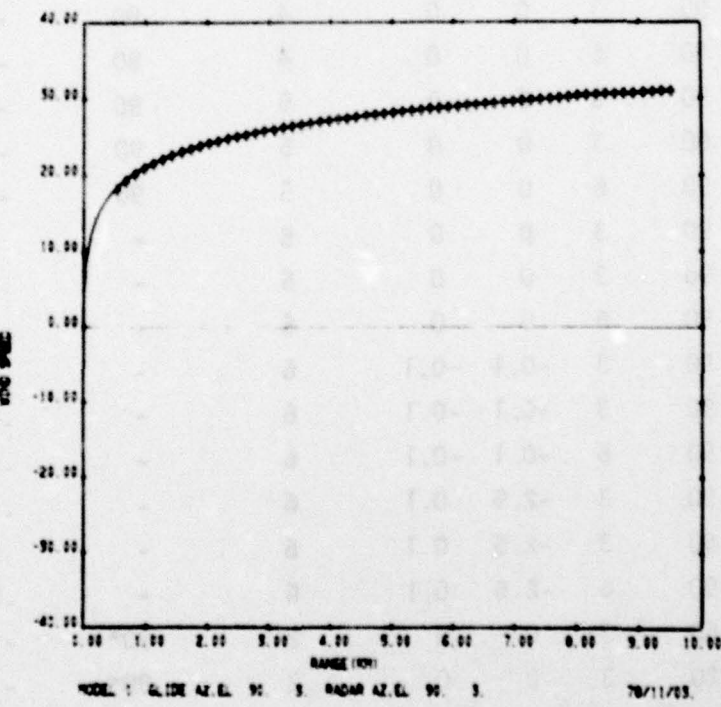


Figure 4.3

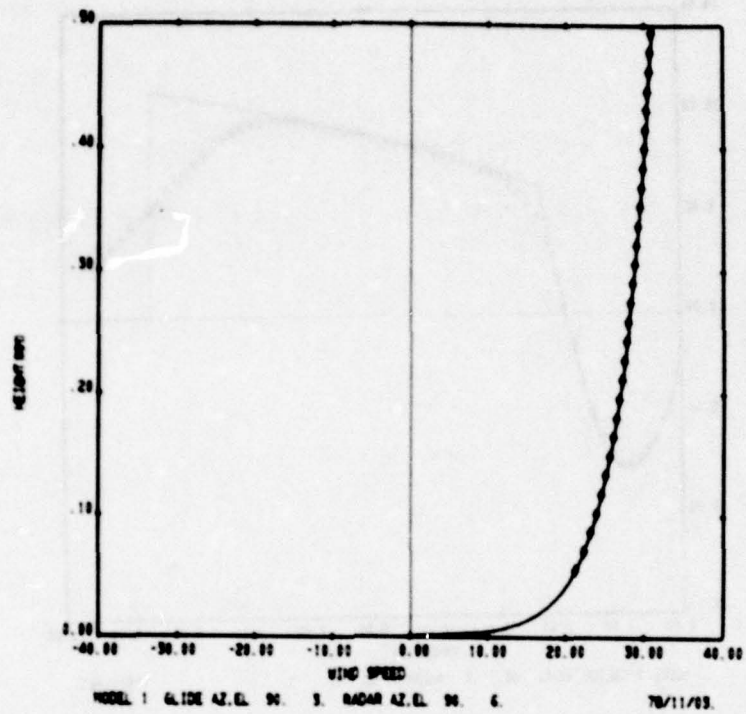


Figure 4.4

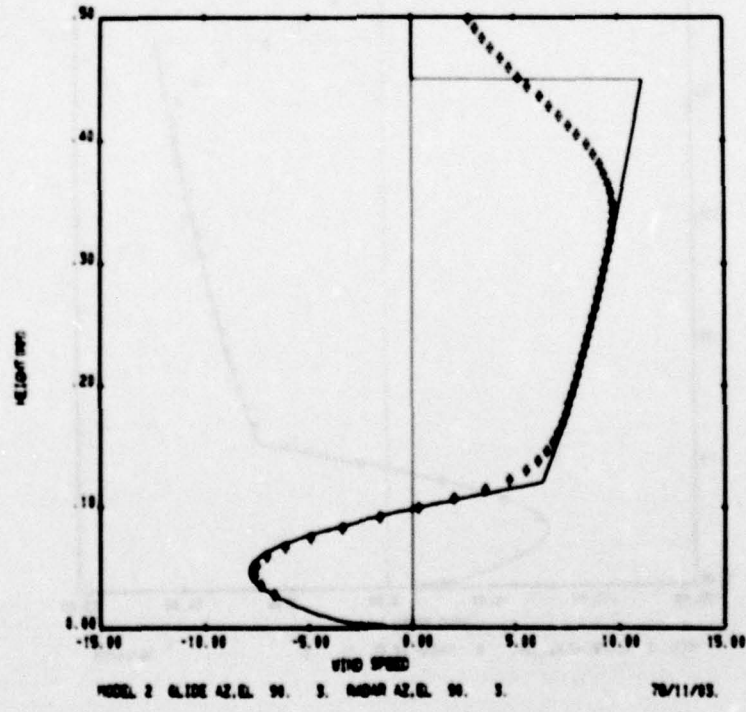


Figure 4.5

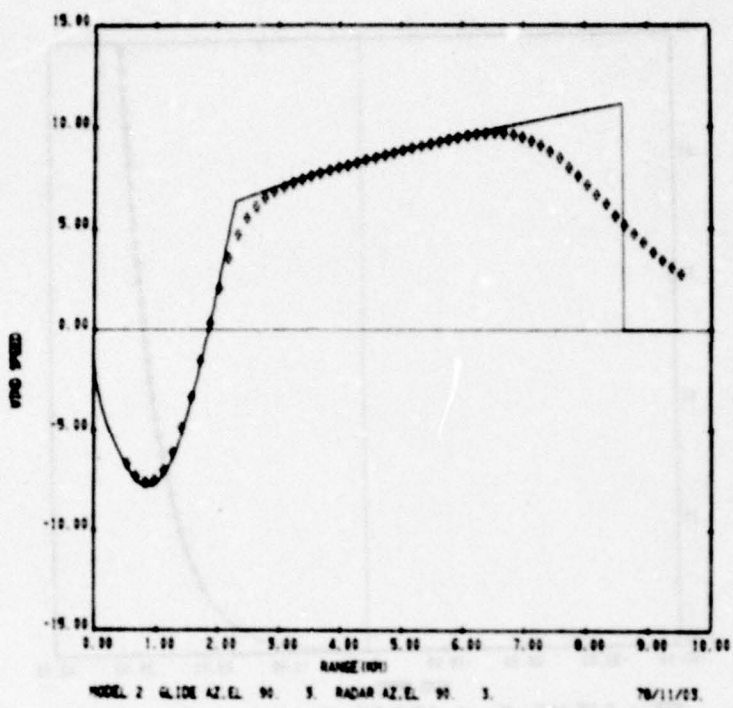


Figure 4.6

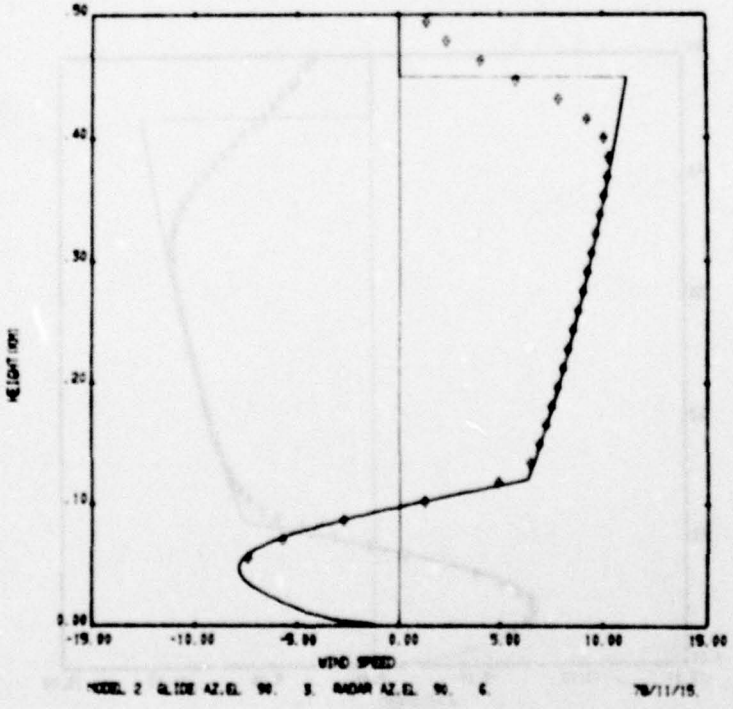


Figure 4.7

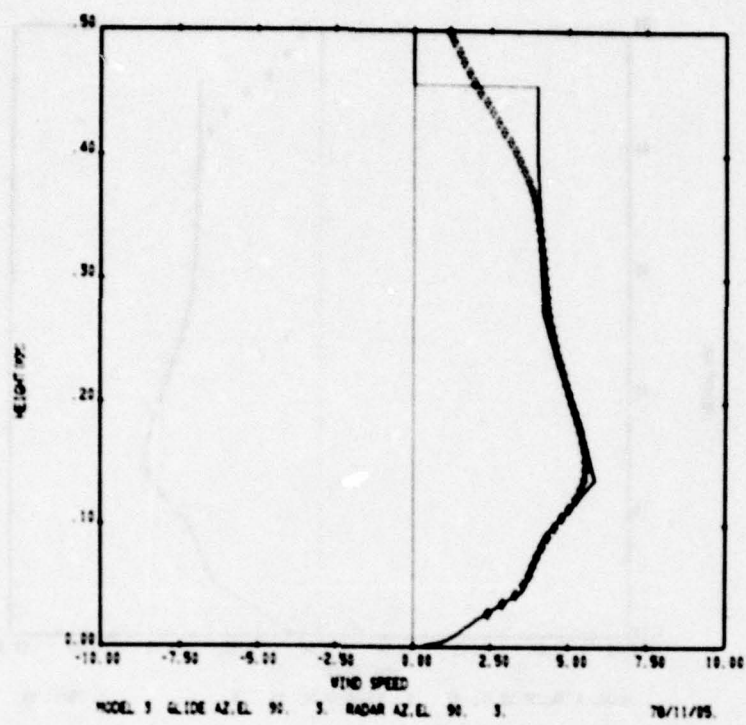


Figure 4.8

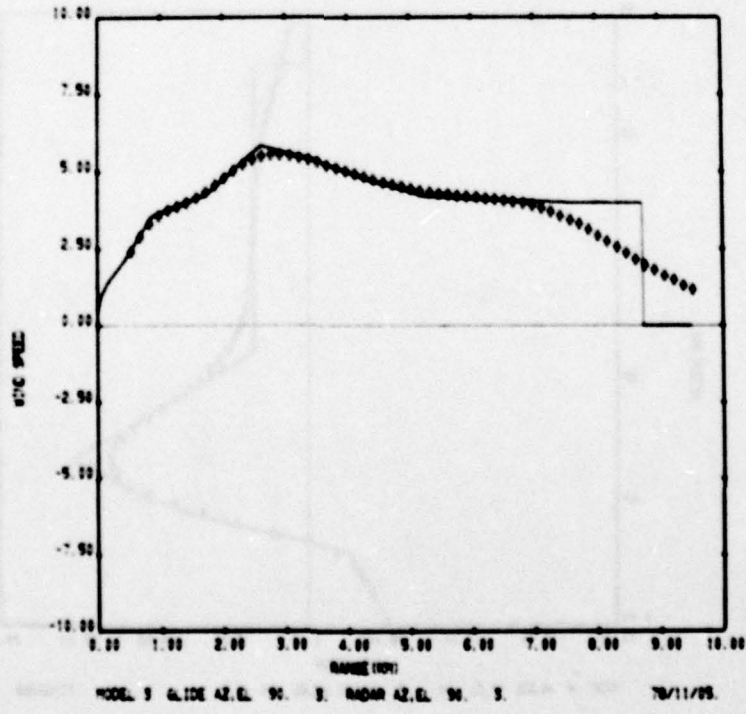


Figure 4.9

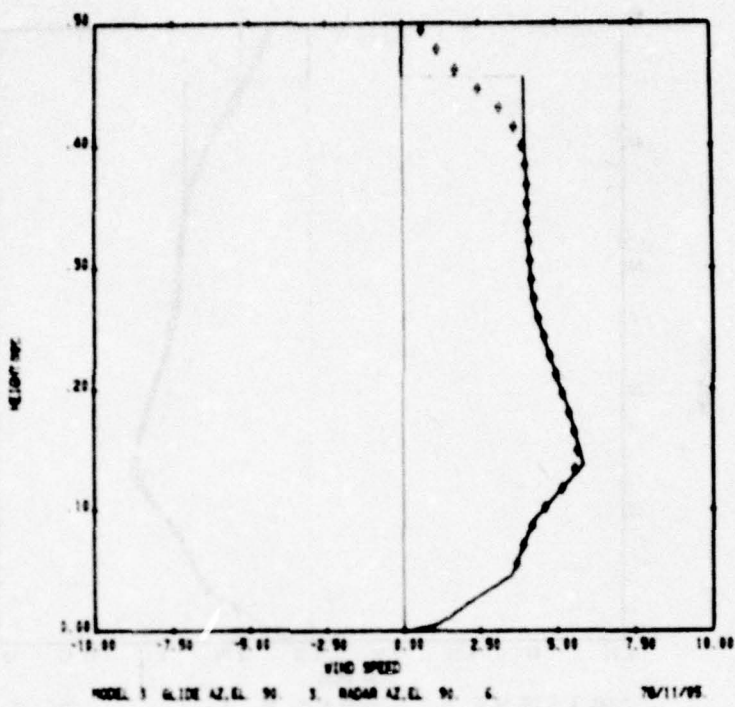


Figure 4.10

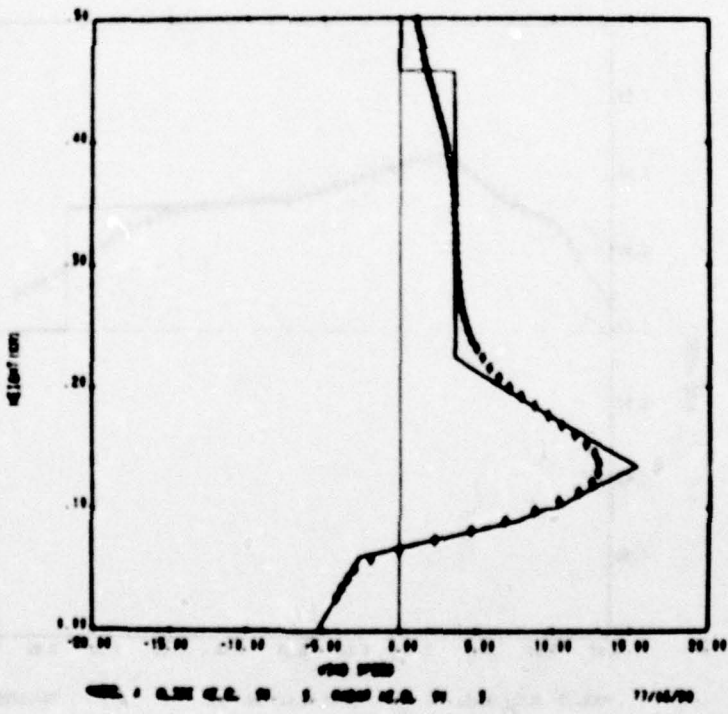


Figure 4.11

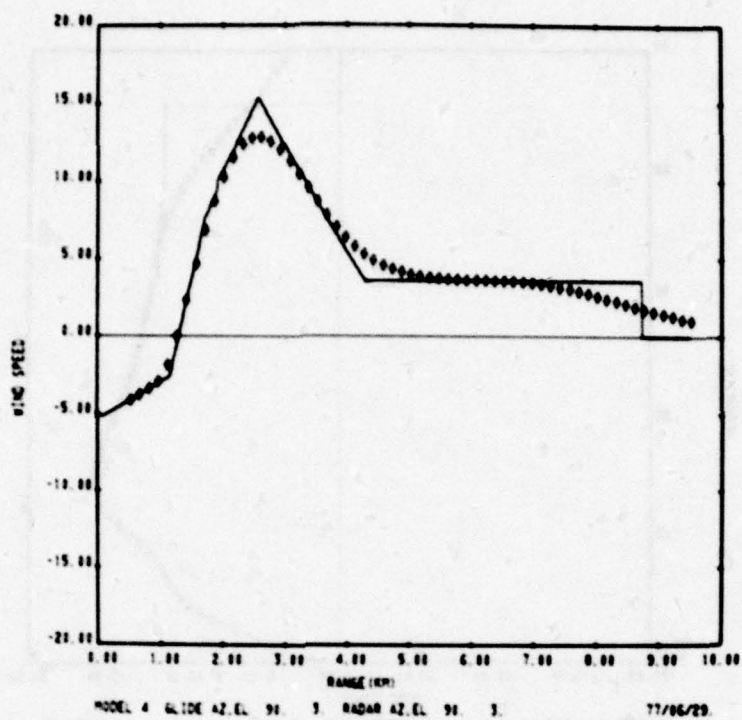


Figure 4.12

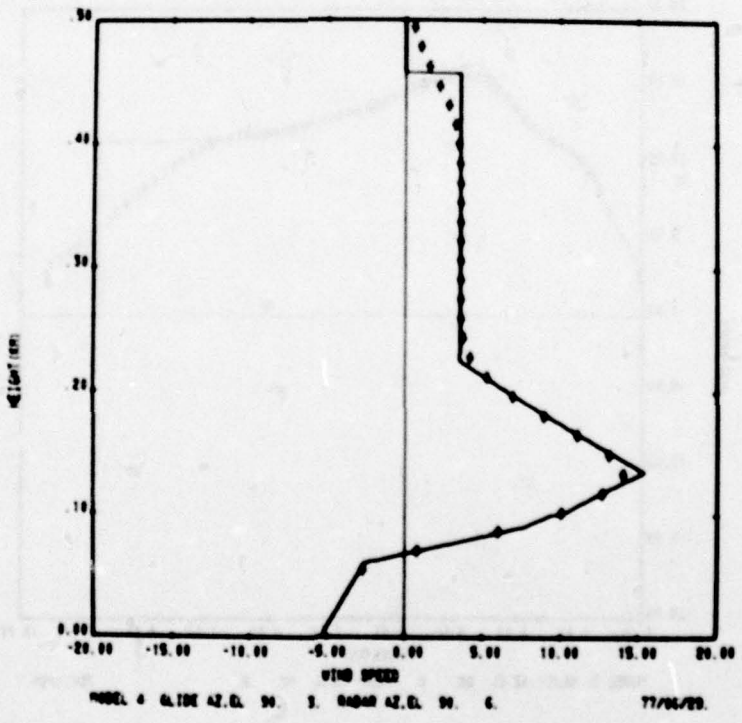


Figure 4.13

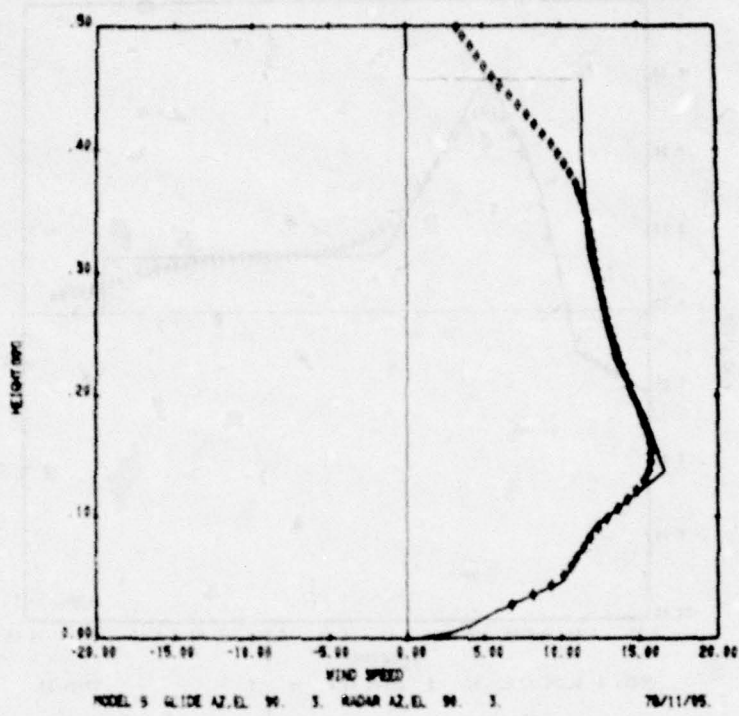


Figure 4.14

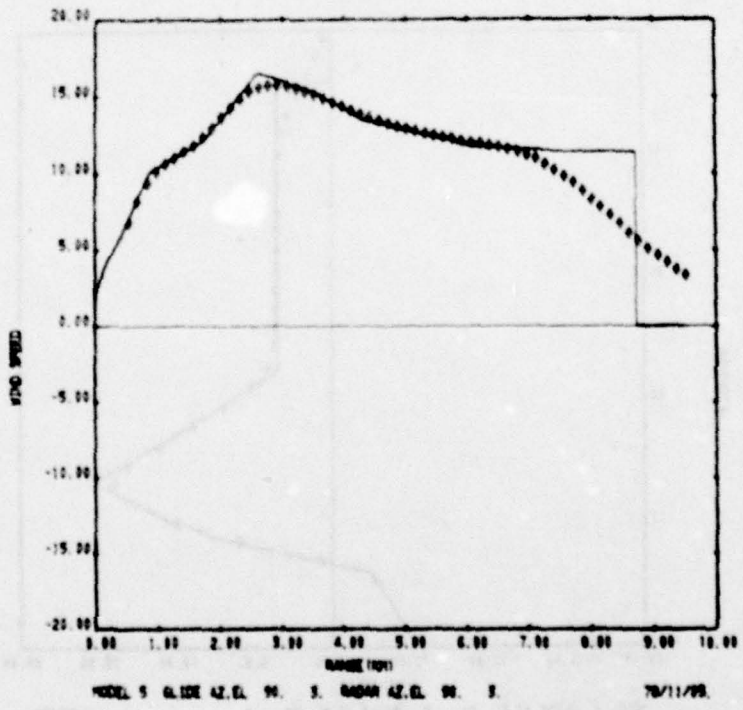


Figure 4.15

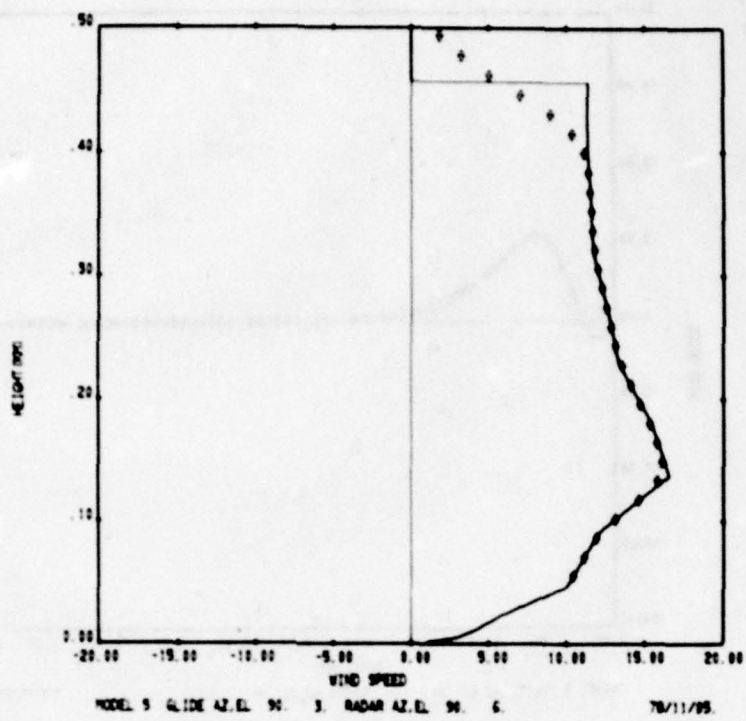


Figure 4.16

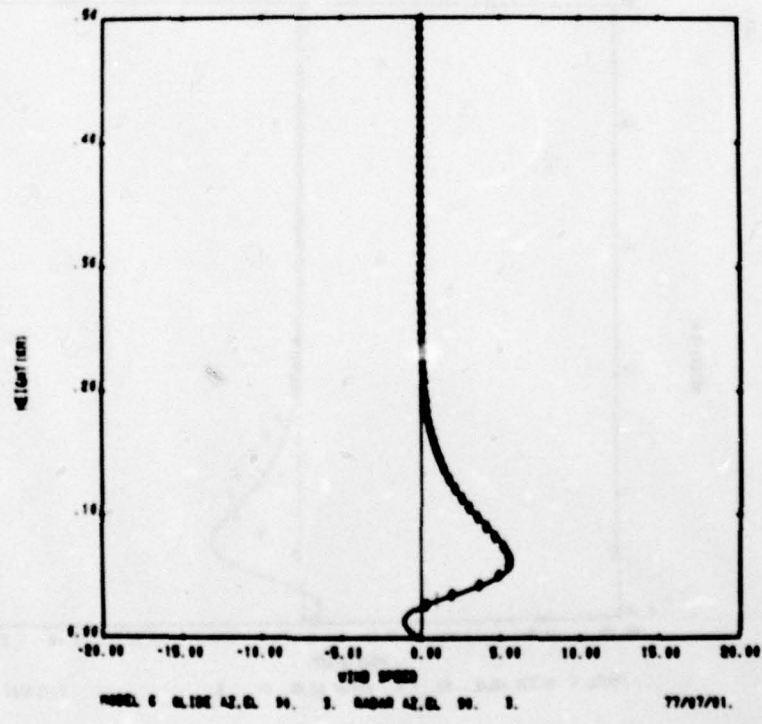


Figure 4.17

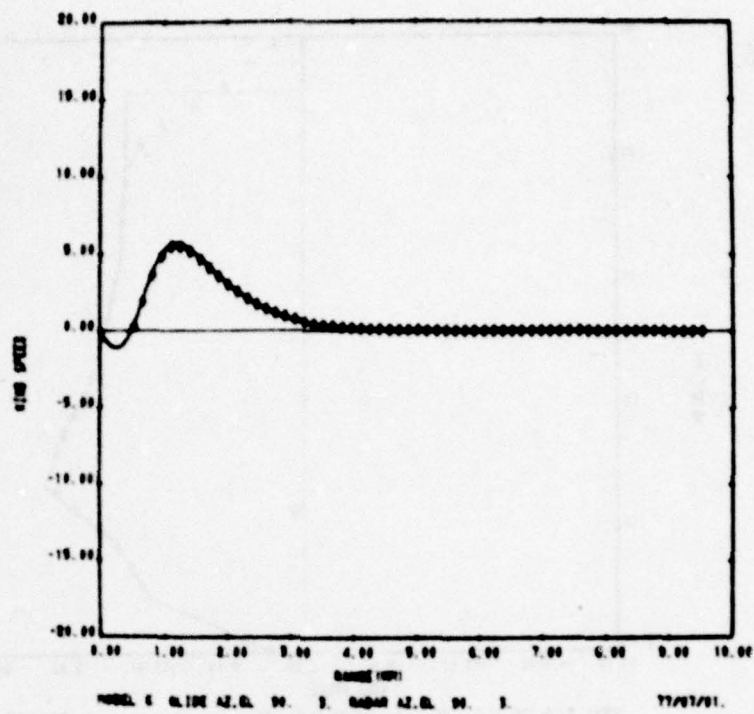


Figure 4.18

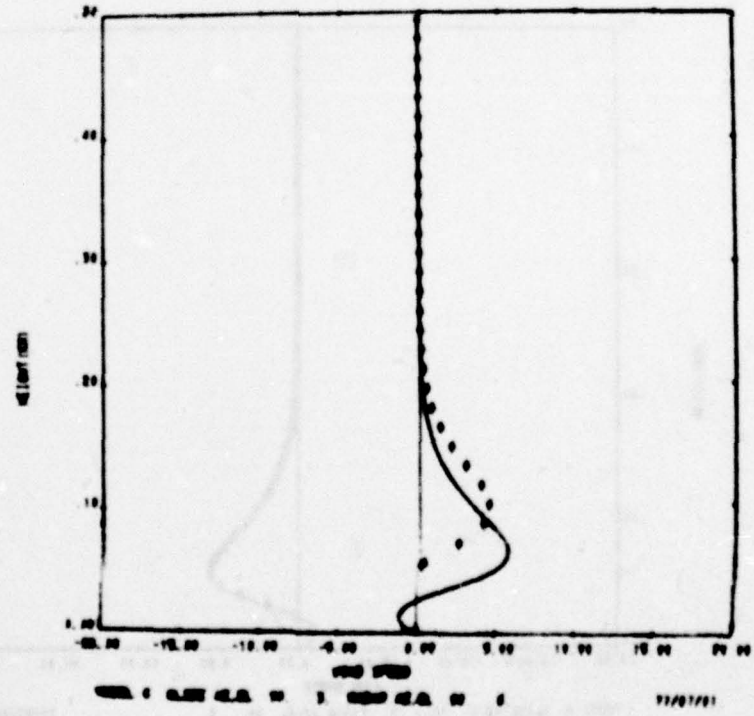


Figure 4.19

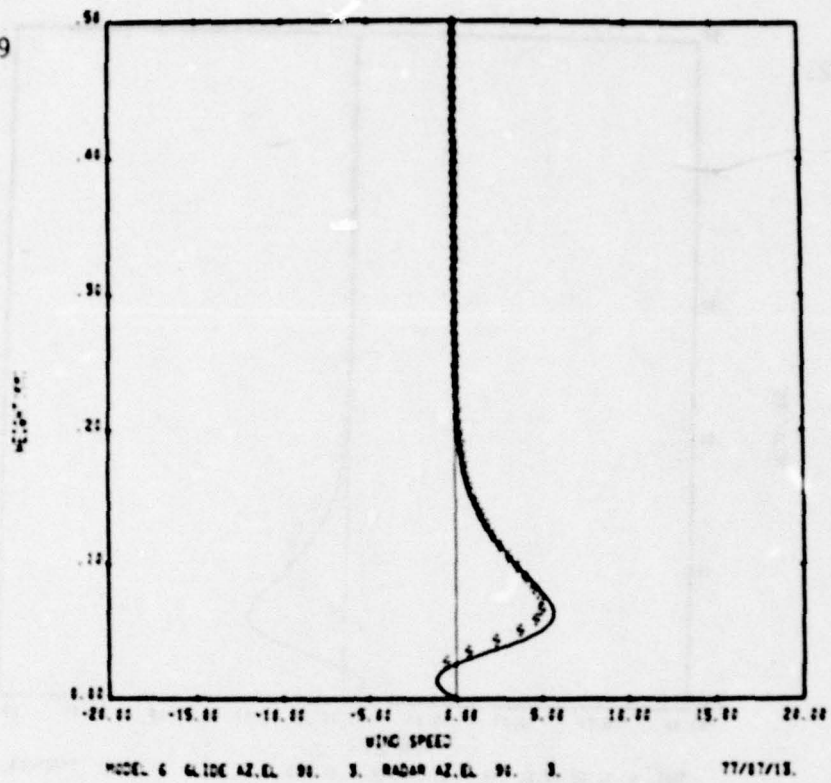


Figure 4.20

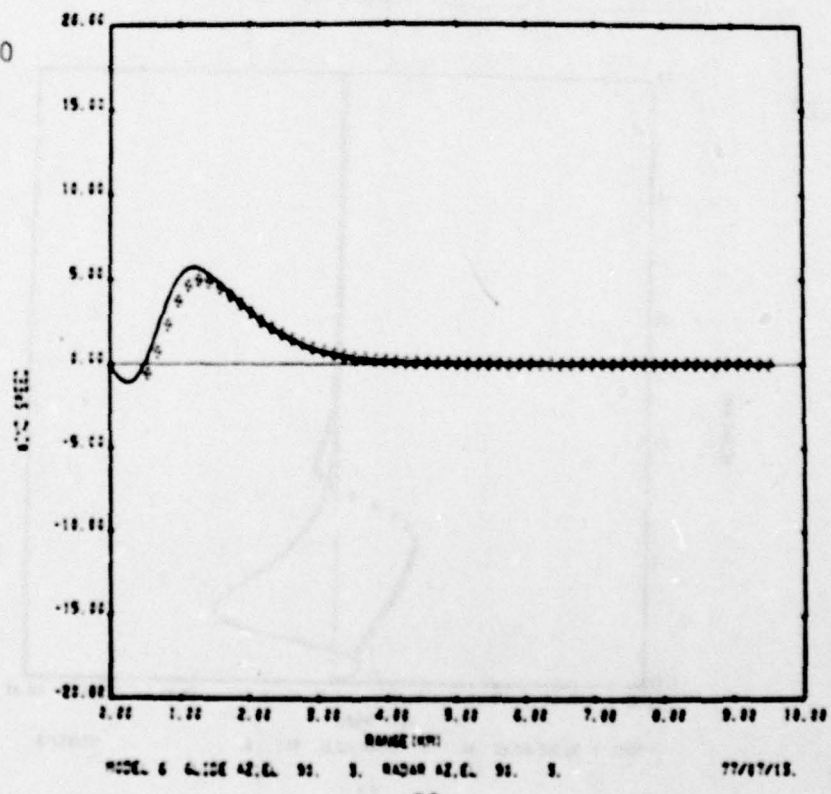


Figure 4.21

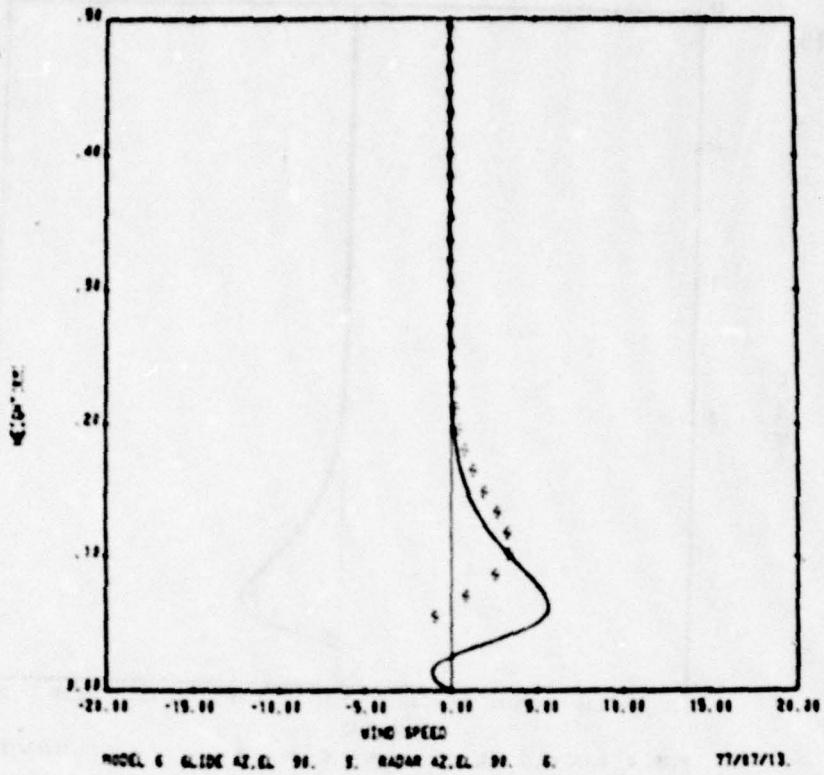


Figure 4.22

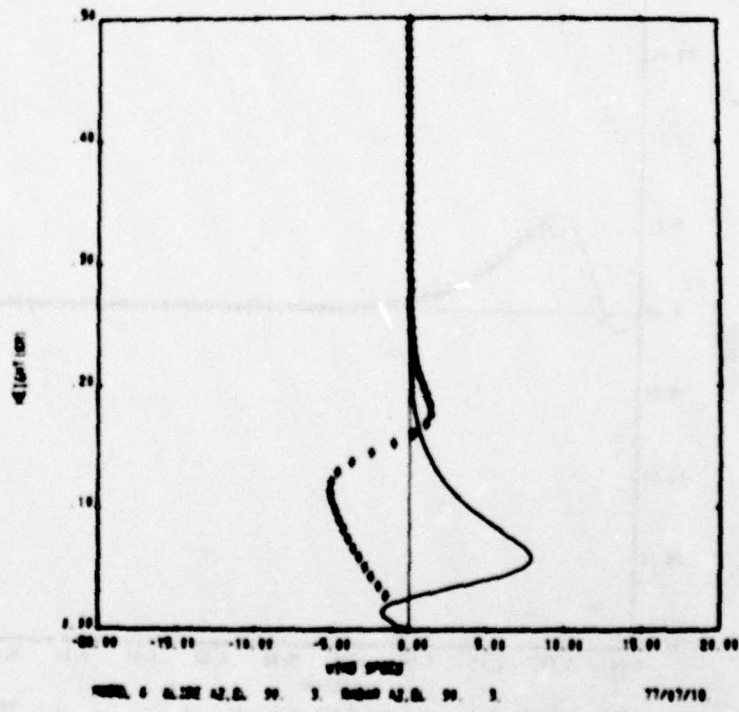


Figure 4.23

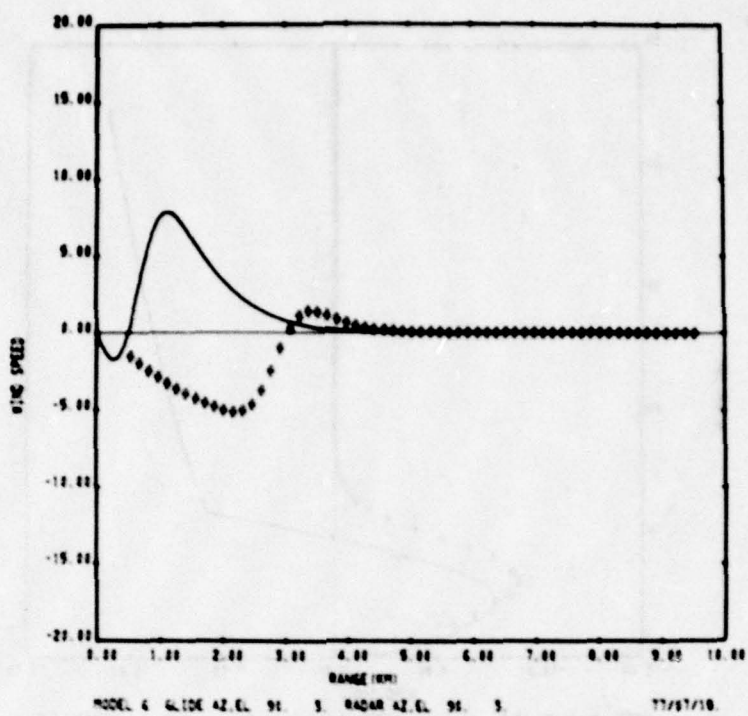


Figure 4.24

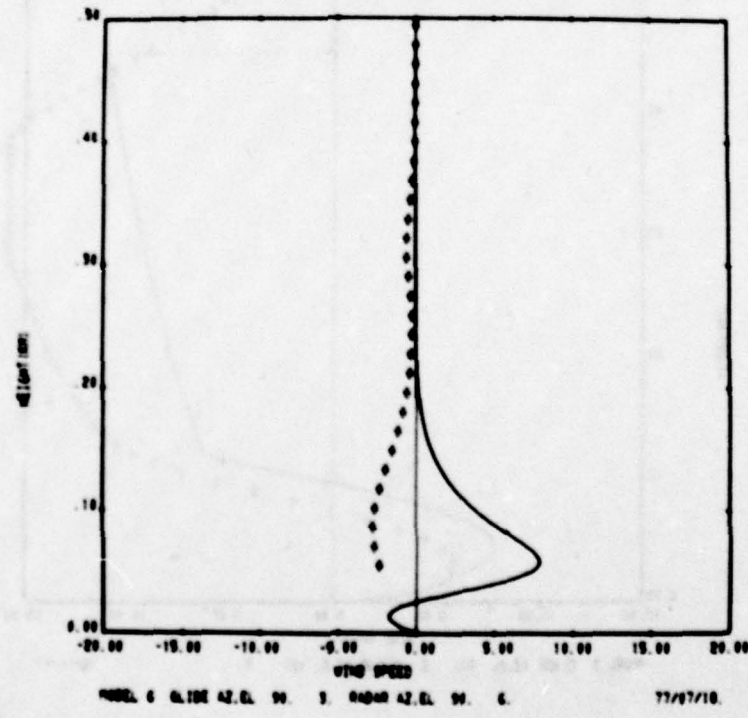


Figure 4.25

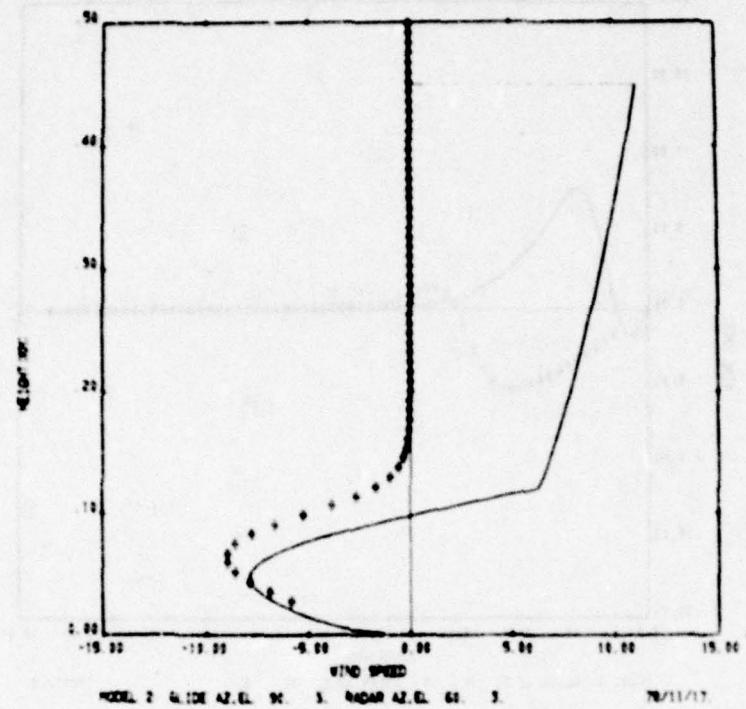
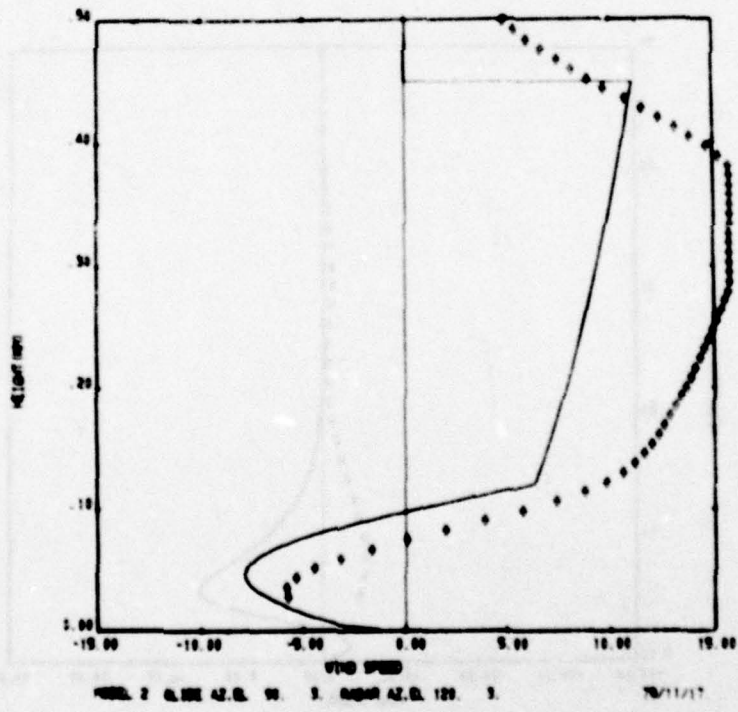


Figure 4.26



Profile 1 (Figures 4.1 through 4.3) has very small gradients, so the radar has no problem measuring this profile.

Profile 2 (Figures 4.4 through 4.6) illustrates the limitations imposed by antenna beamwidth. The large gradients near the 100-m altitude are represented reasonably well by the radar measurements, but the gradient at the top of the input profile is not. This is because the range at the top of the profile is approximately 9 km and the beamwidth is about 235 m. The gradient at 1500 feet is smoothed by the 235-m vertical extent of the radar beam. The effect of pulse length on the filtering of the gradient is negligible since the 150-m range resolution covers only an 8-m altitude change at 3° elevation angle.

Profile 3 (Figures 4.7 through 4.9) again illustrates the problem of measuring large gradients at long range.

Profile 4 (Figures 4.10 through 4.12) contains large low-level gradients (as might be expected from a thunderstorm) as well as discontinuities at mid-level and at the top of the profile. The distance or height interval perturbed by the discontinuity increases with range or height because of filtering by the antenna beamwidth.

Profile 5 (Figures 4.13 through 4.15) again illustrates the ability of the radar to measure wind profiles, except near discontinuities or large gradients.

In all of these profiles, the results for a 6-degree elevation angle are approximately the same as for 3 degrees. The major difference is that for a 6-degree elevation the minimum altitude is doubled (46 m) and the range at maximum altitude is halved, so that large gradients are not filtered as much. If there are significant horizontal gradients present in the wind field, the radar-measured radial velocity profiles

would be different for various elevation angles. Measurement of the profile at the 3-degree and 6-degree elevations can be used to test for important horizontal gradients.

Model 6, a thunderstorm downburst model, contains horizontal gradients of the horizontal wind that show the problems associated with radar location. The figures are also in groups of three with the same display as used above. Results are shown for an input profile that places the location of the downburst near the touchdown point.

In Figures 4.16 through 4.18, the radar location is at the touchdown point with the downburst offset 707 m ( $X_c = Y_c = 500$  m). Figures 4.16 and 4.17 show that the radar can measure the profile when the radar beam is along the 3-degree glide slope; however when the antenna elevation angle is 6-degrees (Figure 4.18), the radar observes a significantly different part of the downburst at every height, and the measured profile deviates from the actual profile along the glide slope.

Figures 4.19 through 4.21 show the results when the radar is displaced by 100 m from the touchdown point in both x and y ( $X_R = Y_R = -100$  m), while the downburst is centered at  $X_c = Y_c = +500$  m. The 3-degree glide slope profiles (Figures 4.19 and 4.20) differ only slightly from the actual profile, while the 6-degree elevation angle profile deviates significantly as before. Displacement of the radar to  $X_R = Y_R = +100$  m (profiles not shown) also shows a small deviation of the radar-measured profile from the actual profile.

However, when more realistic radar offset positions are used ( $X_R = -2.5$  km,  $Y_R = 0.1$  km), the radar-measured profiles (Figures 4.22 through 4.24) do not even resemble the input profiles. At every height, the radar observation is made several kilometers from the glide slope and the result is unacceptable for gradients expected in thunderstorms. For

offset positions this large, the radar would have to be scanned in azimuth or elevation or both so that the radar measurements would be close to the aircraft track. When the radar antenna pointing direction is changed so the radar pulse volume intersects the glide slope, the radar-measured velocities approximate the headwind encountered by the aircraft unless the angle between the radar beam and the aircraft track becomes too large.

When the horizontal gradients can be neglected (as in profiles 1 through 5), both headwind and crosswind can be measured, either by rotating the antenna through a complete revolution (the VAD technique) or by measuring the profile at two angles, (Figures 4.25 and 4.26). The wind input is profile 2, which has crosswind as well as headwind. The antenna elevation angle is 3 degrees. Figure 4.25 shows the measured profile for an azimuth angle 30 degrees counterclockwise from the glide path; the wind direction is perpendicular to this azimuth angle for altitudes greater than 400 feet. Figure 4.26 shows the profile for an azimuth angle 30 degrees clockwise from the glide path. At each height, the headwind is the sum of the two radar measurements divided by  $2\cos(30^\circ)$ , and the crosswind is the difference of the two measurements divided by  $2\sin(30^\circ)$ . (Note that in Figure 4.26 the radar-measured points are off-scale and not properly represented between 250 and 450 m altitude.)

## 5. CONCLUSIONS

The simulation program is described and listed in the Appendix. It can be used to find the expected radar-measured radial velocity profile for any antenna position, beamwidth, pulse length, or radar location. The wind input can be any analytical model. At present, the only output is the radial velocity profile, but the program could be expanded to test scanning strategies that would combine the outputs from various antenna pointing directions to deduce wind profiles.

The simulation results show that for an antenna beamwidth of 1.5 degrees low-level gradients in realistic wind profiles will be properly measured by the radar. If the wind field does not contain significant horizontal gradients, the elevation angle is not critical. The results suggest that one way to test whether horizontal gradients are important is to measure the profile at various elevation angles. At an elevation angle equal to the glide slope (nominally 3 degrees), strong gradients at a 500-m altitude will be heavily filtered by the radar pulse volume, because of the vertical extent of the antenna beamwidth. Therefore, this strong filtering will remain until the elevation angle is very high, and, since the minimum range of a pulse radar is at least several microseconds, it will not be possible to resolve strong gradients at altitudes above several hundred meters. The antenna beamwidth filters the wind profile, but does not significantly filter realistic wind profiles at low levels.

The effect of radar offset from the runway presents a serious problem for wind fields with significant horizontal gradients commonly found in thunderstorms. It is evident from these simulations that the profile along a path parallel to the glide path is not acceptable for offsets of several kilometers. If there is a precipitation echo, the entire region may be scanned (rapidly) and a single Doppler radar may be able to

identify hazardous areas without actually measuring the wind vector. For example, a contoured display of the radar-measured radial velocity (obtained from data acquired during an azimuth sector scan) would reveal the location of the downburst in model 6. Figure 5.1 shows the radial velocity profiles measured by a radar scanning a downburst at several azimuths. In this case the downburst (model 6) is located 2.5 km from the runway ( $X_c = 2.5$  km,  $Y_c = 0$ ), while the radar is located at  $X_R = -2.5$  km,  $Y_R = -0.1$  km. The elevation angle is only 1-degree, so the radar can detect the strong outflow that occurs in the lowest 200 m.

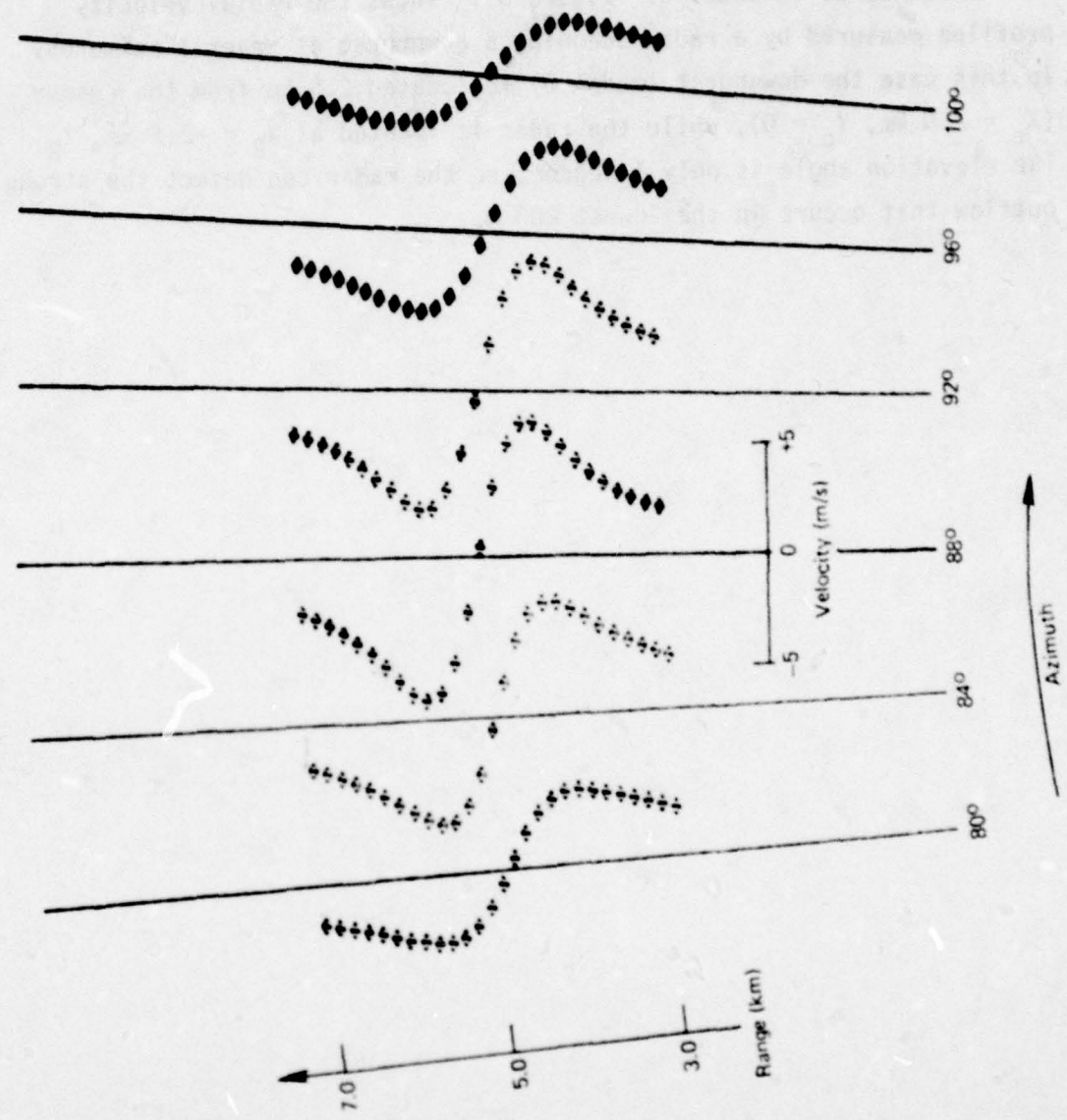


Figure 5.1 Radar-measured radial velocity profiles for a downburst (model 6).  
 $EL = 1$  degree;  $X_C = 2.5$  km;  $Y_C = 0$  km;  $X_R = -2.5$  km;  $Y_R = -0.1$  km.

## APPENDIX: COMPUTER PROGRAM

### 1. Program Structure

The computer program consists of the modules shown in the structural diagram (Figure A.1). This chart illustrates the hierarchy of the modules and not the sequence of execution (Myers, 1975)<sup>4</sup>. The connecting lines indicate that the module below is called by the one above. The parameters passed between the modules are listed in the input-output table (Table A.1). The interface numbers refer to Figure A.1. The parameters listed under INPUT are passed from the calling module to the one called, and those listed under OUTPUT are returned by the called module. The parameter that determines which wind model is used, MDN, and the graphics parameters are the only ones not included in Table A.1. MDN is passed by means of the common block, MODEL.

The system dependent graphics routines (namely AUTOPLT, DDINIT, and DDEND) referenced in the program listing, and their associated common blocks (LABPL and SIZEPL) have been omitted from this discussion.

### 2. Description of the Program Modules

GUSIM	obtains the wind model number and controls the computation of the wind profiles.
GPPROF	computes the actual radial velocity along the glide path.
RMPROF	computes the radial velocity profile measured by the radar.
RPLOT	plots the actual and measured radial velocity profiles versus range.
ZPLOT	plots the radial velocity profiles versus height.
READGP	obtains the glide path parameters, namely, the elevation angle, the azimuth, the maximum range, and the range increment at which the velocity is computed.

<sup>4</sup> G. J. Myers, *Reliable Software Through Composite Design*, (New York: Petrocelli Charter, 1975.)

READRM obtains the following radar parameters: elevation angle, azimuth, maximum range, range increment (for integration net), radar location, pulse length, range delay, and beamwidth.  
 RNINT computes the radar-measured mean radial velocity within a pulse volume by integrating in range the mean radial velocity in the beam cross section.  
 ELINT computes the mean radial velocity in a beam cross section by integrating with respect to elevation the mean radial velocity in the azimuth beamwidth.  
 AZINT computes the mean radial in the azimuth beamwidth.  
 RADVEL converts the spherical coordinates to Cartesian and computes the radial component of u, v, and w.  
 WINDN computes the wind components u, v, and w at the point (x,y,z) for wind model n.

The radar antenna illumination function,  $W = W_{EL} W_{AZ}$ , where

$$W_{EL} = \exp\left(-\frac{(\phi-EL)^2}{2\Delta^2}\right),$$

and

$$W_{AZ} = \exp\left(-\frac{(\theta-AZ)^2}{2\Delta^2}\right),$$

was factored, so that the integral could be evaluated one step at a time, as follows:

$$V_{AZ} = \frac{\sum V_R W_{AZ}}{\sum W_{AZ}}$$

$$V_{EL} = \frac{\sum V_{AZ} W_{EL}}{\sum W_{EL}}$$

$$V_M = \frac{1}{N} \sum V_{EL}$$

where N is the number of range increments in a pulse. This was done to facilitate programing, but had the added benefit of eliminating the need for large array storage.

STRUCTURAL DIAGRAM

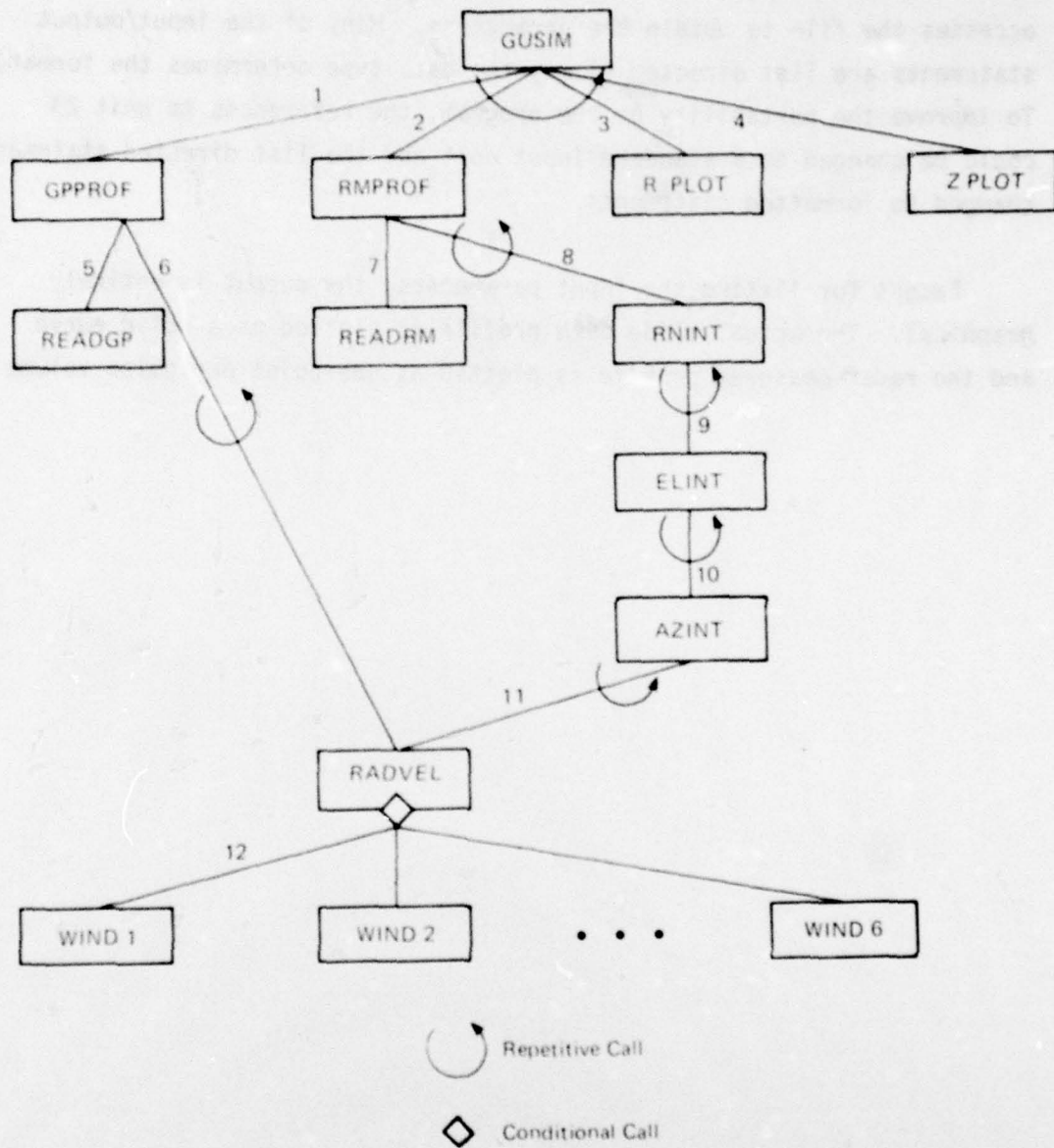


Figure A.1 Structure diagram for the simulation program.

### 3. Data Input-Output

This program has been run in conjunction with an interactive program that interrogates the user to request parameters. The parameters are stored in a file named TAPE23. This program running in batch mode accesses the file to obtain the parameters. Many of the input/output statements are list directed (i.e., the data type determines the format). To improve the portability of the program, the references to unit 23 could be changed to a standard input unit and the list directed statement changed to formatted statements.

Except for listing the input parameters, the output is entirely graphical. The actual glide path profile is plotted as a solid curve and the radar-measured profile is plotted as one-point per pulse volume.

4. Listing

INTER-FACE	INPUT	OUTPUT
1		<p>GPW Glide path radial velocity      GPG Distance along glide path      GPZ Altitude along glide path      NGP Number of points</p>
2		<p>RMW Radar measured radial velocity      RRG Radar range      RMZ Altitude along beam      NRM Number of points</p>
3	GPW,GRG,NPG,RMW,RRG,NRM	
4	GPW,GPZ,NGP,RMW,RMZ,NRM	
5		<p>GPH Glide path azimuth      GPA Glide path elevation angle      GPR Maximum distance along glide path      DRG Distance between points</p>
6	R Same as GRG AZ GPH converted to radians EL GPA in radians	Radial velocity along glide path
7		<p>RAZ Radar azimuth      REL Radar elevation angle      RNG Maximum radar range      DRR Range increment      XR,YR Radar coordinates      RPL Radar pulse length      RRD Radar range delay      RBW Radar beamwidth</p>
8	RRG DRM Pulse length in km. DRR AZ RAZ in radians EL REL in radians XR,YR BW RBW in radians	Mean radial velocity in pulse volume
9	R Same as RRG DRR,AZ,EL,XR,YR,BW	Mean radial velocity in beam cross section
10	R,DRR,AZ,EL,XR,YR,BW	Mean radial velocity with respect to azimuth beamwidth
11	R,AZ,EL,YR,YR	Radial velocity at a point
12	X,Y,Z Coordinates of point	U,V,W Wind components

Table A.1

```

PROGRAM GUSIM(INPUT,OUTPUT,TAPE23)
COMMON/MODEL/MDN
DIMENSION GPW(1001),GRG(1001),GPZ(1001),
X           RMW(101),RRG(101),RMZ(101)
CALL DDINIT(2,20H SWEZY X6462 RB3   )
REWIND 23
1  CONTINUE
NRM = 100
NGP = 1000
READ(23,*)MDN
PRINT*, " MODEL NUMBER ",MDN
IF(MDN.LT.1)GO TO 2
IF(MDN.GT.6)GO TO 2
CALL GPPROF(GPW,GRG,GPZ,NGP)
CALL RMPROF(RMW,RRG,RMZ,NRM)
CALL RPLOT(GPW,GRG,NGP,RMW,RRG,NRM)
CALL ZPLOT(GPW,GPZ,NGP,RMW,RMZ,NRM)
GO TO 1
2  CONTINUE
CALL DDEND
END

SUBROUTINE GPPROF(GPW,GRG,GPZ,NGP)
C   ROUTINE TO COMPUTE RADIAL VELOCITY PROFILE ALONG GLIDE PATH
C   GPW IS RADIAL VELOCITY
C   GRG IS RANGE
C   GPZ IS ALTITUDE
C   NGP IS NUMBER OF POINTS
      DIMENSION GPW(1),GRG(1),GPZ(1)
      CALL READGP(GPH,GPA,GPR,DRG)
C   CONVERT ANGLES TO RADIANS
      AZ = 0.0174533*GPH
      EL = 0.0174533*GPA
      NG = GPR/DRG + 1
      NGP = MIN0(NGP,NG)
      R = 0
      DO 5 K = 1,NGP
          R = R + DRG
          GRG(K) = R
          GPZ(K) = R*SIN(EL)
          GPW(K) = RADVEL(R,AZ,EL,0.0,0.0)
5   CONTINUE
      RETURN
      END

```

```

SUBROUTINE RMPROF(RMW,RRG,RMZ,NRM)
C ROUTINE TO COMPUTE RADAR MEASURED RADIAL VELOCITY PROFILE
C RMW IS RADIAL VELOCITY
C RRG IS RANGE
C RMZ IS ALTITUDE
C NRM IS NUMBER OF POINTS
  DIMENSION RMW(1),RRG(1),RMZ(1)
  CALL READRM(RAZ,REL,RNG,DRR,XR,YR,RPL,RRD,RBW)
C CONVERT ANGLES TO RADIANS
  AZ = 0.0174533*RAZ
  EL = 0.0174533*REL
  BW = 0.0174533*RBW
C CONVERT RANGE TIMES TO KM.
  DRM = 0.15*RPL
  RRG(1) = 0.15*RRD + 0.5*DRM
  RMX = RNG - 0.5*DRM
  K = 0
1  CONTINUE
  K = K + 1
  RMZ(K) = RRG(K)*SIN(EL)
  RMW(K) = RNINT(RRG(K),DRM,DRR,AZ,EL,XR,YR,BW)
  RRG(K+1) = RRG(K) + DRM
  IF(RRG(K).LT.RMX .AND. K.LT.NRM)GO TO 1
  NRM = K
  RETURN
  END

```

```

SUBROUTINE RPLOT(GPW,GRG,NGP,RMW,RRG,NRM)
C ROUTINE TO PLOT ACTUAL GLIDE PATH PROFILE AND RADAR MEASURED
C PROFILE VERSUS RANGE.
  COMMON/LABPL/LABX(8),LABY(8),ID(8)
  COMMON/SIZEPL/XLO,XUP,YLO,YUP,KDX,KDY,KSX,KSY
  DIMENSION GPW(1),SCL(7),KDV(7)
  DATA SCL/0.,5.,10.,15.,20.,30.,40./
  DATA KDV/0.4,8,6,8,6,8/
  LABX(4) = 10HRANGE(KM)
  LABY(4) = 10HWIND SPEED
  XLO = 0.0
  XUP = 10.0
  KDX = 10
  WMX = GPW(1)
  DO 1 J=2,NGP
    WMX = AMAX1(WMX,ABS(GPW(J)))
1  CONTINUE
  DO 2 J=2,7
    IF(WMX.LT.SCL(J-1))GO TO 2
    YUP = SCL(J)
    YLO = -YUP
    KDY = KDV(J)
2  CONTINUE
  KSX = KSY = 1
  CALL AUTOPLT(GRG,GPW,NGP,2,8,1)
  CALL AUTOPLT(RRG,RMW,NRM,2,-58,0)
  RETURN
  END

```

```

SUBROUTINE ZPLOT(GPW,GPZ,NGP,RMW,RMZ,NRM)
C ROUTINE TO PLOT ACTUAL GLIDE PATH PROFILE AND RADAR MEASURED
C PROFILE VERSUS HEIGHT.
COMMON/LABPL/LABX(8),LABY(8),ID(8)
COMMON/SIZEPL/XLO,XUP,YLO,YUP,KDX,KDY,KSX,KSY
DIMENSION GPW(1),SCL(7),KDV(7)
DATA SCL/0.,5.,10.,15.,20.,30.,40./
DATA KDV/0.,4.,8.,6.,8.,6.,8./
LABY(4) = 10HHEIGHT(KM)
LABX(4) = 10HWIND SPEED
WMX = GPW(1)
DO 1 J=2,NGP
  WMX = AMAX1(WMX,ABS(GPW(J)))
1 CONTINUE
DO 2 J=2,7
  IF(WMX.LT.SCL(J-1))GO TO 2
  XUP = SCL(J)
  XLO = -XUP
  KDX = KDV(J)
2 CONTINUE
YLO = 0.
KDY = 5
YUP = 0.5
KSX = KSY = 1
CALL AUTOPLT(GPW,GPZ,NGP,2,8,1)
CALL AUTOPLT(RMW,RMZ,NRM,2,-58,0)
RETURN
END

```

```

SUBROUTINE READGP(GPH,GPA,GPR,DRG)
C GLIDE PATH PARAMETER INPUT ROUTINE
COMMON/LABPL/LABX(8),LABY(8),ID(8)
COMMON/MODEL/MDN
READ(23,*)GPH,GPA,GPR,DRG
PRINT*, " GLIDE PATH HEADING-180 (AZIMUTH) ",GPH,"DEG."
PRINT*, " GLIDE PATH ANGLE (ELEVATION) ",GPA,"DEG."
PRINT*, " MAX RANGE ",GPR,"KM."
PRINT*, " RANGE INCREMENT ",DRG,"KM."
ENCODE(30,1002,ID)MDN,GPH,GPA
1002 FORMAT("MODEL" I2" GLIDE AZ,EL" 2F5.0)
RETURN
END

```

```

        SUBROUTINE READRM(RAZ,REL,RNG,DRR,XR,YR,RPL,RRD,RBW)
C   RADAR PARAMETER INPUT ROUTINE
    COMMON/LABPL/LABX(8),LABY(8),ID(8)
    READ(23,*)RAZ,REL,RNG,DRR,XR,YR,RPL,RRD,RBW
    PRINT 1002,RAZ
1002 FORMAT(* RADAR AZIMUTH ANGLE *F4.0*DEG.*)
    PRINT 1004,REL
1004 FORMAT(* RADAR ELEVATION ANGLE *F3.0*DEG.*)
    PRINT 1006,RNG
1006 FORMAT(* MAX RADAR RANGE *F4.1*KM.*)
    PRINT 1008,DRR
1008 FORMAT(* RANGE SAMPLING INCREMENT *F4.2*KM.*)
    PRINT 1010,XR,YR
1010 FORMAT(* RADAR DISPLACEMENT(X,Y) FROM TOUCHDOWN (*
X      F4.2*,*F4.2*)KM.*)
    PRINT 1012,RPL
1012 FORMAT(* RADAR PULSE LENGTH *F3.1*MICROSEC.*)
    PRINT 1014,RRD
1014 FORMAT(* RADAR RANGE DELAY *F3.1*MICROSEC.*)
    PRINT 1016,RBW
1016 FORMAT(* RADAR BEAM WIDTH *F3.1*DEG.*)
    ENCODE(23,2002,ID(4))RAZ,REL
2002 FORMAT(* RADAR AZ,EL*2F5.0)
    RETURN
    END

```

```

        FUNCTION RNINT(RRG,DRM,DRR,AZ,EL,XR,YR,BW)
C   COMPUTES MEAN RADIAL VELOCITY IN PULSE VOLUME BY INTEGRATING,
C   WITH RESPECT TO RANGE, THE MEAN VELOCITY WITH RESPECT TO BEAM WIDTH
    R = RRG - 0.5*DRM
    RMX = R + DRM
    SV = 0.
    EN = 0.
1   CONTINUE
    VR = ELINT(R,DRR,AZ,EL,XR,YR,BW)
    SV = SV + VR
    EN = EN + 1.
    R = R + DRR
    IF(R.LE.RMX)GO TO 1
    RNINT = SV/EN
    RETURN
    END

```

```

        FUNCTION ELINT(R,DRR,AZ,EL,XR,YR,BW)
C   COMPUTES MEAN RADIAL VELOCITY ACROSS BEAM BY INTEGRATING,
C   WITH RESPECT TO ELEVATION ANGLE, THE MEAN VELOCITY WITH RESPECT TO
C   AZIMUTH
        DELTA = 0.3*BW
        ANG = 3.14*DELTA
        DEL = DRR/(R*COS(EL))
        VL = AZINT(R,DRR,AZ,EL,XR,YR,BW)
        DL = 0.
        D2 = 2.*DELTA*DELTA
        SW = 1.
1      CONTINUE
        DL = DL + DEL
        ELP = EL + DL
        ELM = EL - DL
        VP = AZINT(R,DRR,AZ,ELP,XR,YR,BW)
        VM = AZINT(R,DRR,AZ,ELM,XR,YR,BW)
        WT = EXP(-DL*DL/D2)
        SW = SW + 2.*WT
        VL = VL + WT*(VP+VM)
        IF(DL.LT.ANG)GO TO 1
        ELINT = VL/SW
        RETURN
        END

```

```

        FUNCTION AZINT(R,DRR,AZ,EL,XR,YR,BW)
C   COMPUTES MEAN RADIAL VELOCITY WITH RESPECT TO AZIMUTH
        DELTA = 0.3*BW
        ANG = 3.14*DELTA
        DAZ = DRR/R
        VL = RADVEL(R,AZ,EL,XR,YR)
        DA = 0.
        D2 = 2.*DELTA*DELTA
        SW = 1.
1      CONTINUE
        DA = DA + DAZ
        AZP = AZ + DA
        AZM = AZ - DA
        VP = RADVEL(R,AZP,EL,XR,YR)
        VM = RADVEL(R,AZM,EL,XR,YR)
        WT = EXP(-DA*DA/D2)
        SW = SW + 2.*WT
        VL = VL + WT*(VP+VM)
        IF(DA.LT.ANG)GO TO 1
        AZINT = VL/SW
        RETURN
        END

```

```

FUNCTION RADVEL(R,AZ,EL,XR,YR)
C COMPUTES RADIAL VELOCITY COMPONENT OF U,V,W FOR A GIVEN WIND MODEL
COMMON/MODEL/MDN
SA = SIN(AZ)
CA = COS(AZ)
SE = SIN(EL)
CE = COS(EL)
X = R*CE*SA + XR
Y = R*CE*CA + YR
Z = AMAX1(0.0,R*SE)
IF(MDN.EQ.1)CALL WIND1(X,Y,Z,U,V,W)
IF(MDN.EQ.2)CALL WIND2(X,Y,Z,U,V,W)
IF(MDN.EQ.3)CALL WIND3(X,Y,Z,U,V,W)
IF(MDN.EQ.4)CALL WIND4(X,Y,Z,U,V,W)
IF(MDN.EQ.5)CALL WIND5(X,Y,Z,U,V,W)
IF(MDN.EQ.6)CALL WIND6(X,Y,Z,U,V,W)
RADVEL = (U*SA + V*CA)*CE + W*SE
RETURN
END

```

```

SUBROUTINE WIND 1(X,Y,Z,U,V,W)
C THIS VERSION GENERATES U GIVEN Z
C THIS PROFILE IS FOR NO VARIATION OF WIND DIRECTION WITH ALTITUDE
C .00045.LE.Z.LE..45KM. (1.5.LE.Z.LE.1500FT.)
C U20 IS WIND AT 20FT. ALTITUDE
C NOMINAL VALUE = 5 M/S
C FOR REFERENCE, CONSTANTS DEFINED AND FORMULA GIVEN IN FEET
C IF(Z.LT.1.5) GO TO 600
C DLOG13=LN 13.33
C ZLOG15=LN (Z/1.5)
C U=U20*ZLOG15/DLOG13
  U006=11.5
  U=0
  W=0
  V=0
  IF(Z.LT..00045) GO TO 600
  DLOG13=2.590017134
  ZLOG15= ALOG(Z/.00045)
  U=U006*ZLOG15/DLOG13
  RETURN
600  U=0
  RETURN
END

```

```
SUBROUTINE WIND 2(X,Y,Z,U,V,W)
C THIS VERSION GENERATES U, V FOR GIVEN Z
C WHERE 0.LE.Z.LE.0.45KM.
C NOMINAL VALUE OF U006 IS 5 M/S
C THETO IS SURFACE WIND (.006 KM.) DIRECTION
  THETO=180.
  U=0
  V=0
  W=0
  IF(Z.LE.0.0)RETURN
C FOR WIND SPEED WE HAVE,
C U006 IS WIND AT .006 KM.
  U006=3.5
  UU=U006*(Z/.006)**0.43
C FOR WIND DIRECTION WE HAVE,
  IF((.12.LE.Z).AND.(Z.LE..45)) GO TO 14
  IF((.03.LE.Z).AND.(Z.LE..12)) GO TO 15
  IF((0.LE.Z).AND.(Z.LE..03)) GO TO 16
C MODEL FAILS FOR THIS Z
  RETURN
14  THET=120+THETO
  GO TO 17
15  THET=120.*(Z-.03)/.09 + THETO
  GO TO 17
16  THET=THETO
17  U=UU*COS(THET/57.3)
  V=UU*SIN(THET/57.3)
  RETURN
  END
```

```

      SUBROUTINE WIND 3(X,Y,Z,U,V,W)
C THIS PROFILE IS THUILLIER/LAPPE NUMBER 5
C FOR NIGHTTIME STABLE LAYER BOUNDARY
C EXPECTS DISTANCE IN KILOMETERS GIVES U IN METER/SECOND
C U009 IS VELOCITY AT .0091 KM.
      DIMENSION UZ(12),Z0(12)
      DATA (UZ=1.389,2.109,3.550,4.270,5.866,5.403,4.734,4.219,4.116,
&4.065,4.013,4.013)
      DATA (Z0=.0091,.0228,.0457,.0914,.1371,.1828,.2286,.2743,.3200,
&.3657,.3962,.4572)
C FIND HEIGHT INTERVAL I
      U009=UZ(1)
      U=V=W=0.
      IF(Z.LE.0.0)RETURN
      DO 80 J=1,12
      K=J
      IF(Z.LT.Z0(J)) GO TO 85
80  CONTINUE
C MODEL FAILS FOR THIS Z.
      RETURN
85  I=K
      IF(I.GT.1) GO TO 3
2    U=U009*(Z/.0091)**.45
      RETURN
C DO LINEAR INTERPOLATION FOR I=2,12
3    UZ1=UZ(I)
      UZ2=UZ(I-1)
      Z01=Z0(I)
      Z02=Z0(I-1)
      U=UZ2-(Z02-Z)*(UZ2-UZ1)/(Z02-Z01)
      RETURN
END

```

```

        SUBROUTINE WIND 4(X,Y,Z,U,V,W)
C THIS PROFILE IS FOR THUNDERSTORM COLD AIR OUTFLOW
C EXPECTS DISTANCE IN KILOMETERS GIVES U,V,W IN METER/SECOND
C THIS PROFILE GIVES W, GIVEN Z
C FOR W, THERE ARE 4 CASES; MAJOR AND MINOR UPDRAFTS AND DOWNDRAFTS.
C CONSTANTS USED IN THIS MODEL ARE; ZD,ZR,A,L,P1,P2,Q0,Q1,Q2.
C VALUES FOR ZD,ZR,L ARE IN KM.,A IS IN METER/SECOND
        DIMENSION VZ(7),UZ(7),Z0(7)
        DATA (UZ=-5.1328,-5.1328,-2.5664,7.6992,15.3984,3.5929,3.5929)
        DATA (VZ=1.5398,1.5398,4.1062,4.1062,5.1328,6.6726,5.1328)
        DATA (Z0=0,.0061,.0609,.0900,.1350,.2250,.4572)
        DATA ZD,ZR,XL,A,P1,P2,Q0,Q1,Q2/.2347,.1371,.0396,4.2672,
&1.21,0.36,-0.36,2.4165,1.0769/
        U=V=W=0
        IF(Z.LE.0.0)RETURN
C FIND HEIGHT INTERVAL I
        DO 80 J=1,7
        K=J
        IF(Z.LT.Z0(J)) GO TO 85
80    CONTINUE
C MODEL FAILS FOR THIS Z
        RETURN
85    I=K
        IF(I.GT.1) GO TO 3
2    U=-5.1328
V=1.5398
        GO TO 49
C DO LINEAR INTERPOLATION FOR I=2,12
3    UZ1=UZ(I)
        UZ2=UZ(I-1)
        VZ1=VZ(I)
        VZ2=VZ(I-1)
        Z01=Z0(I)
        Z02=Z0(I-1)
        U=UZ2-(Z02-Z)*(UZ2-UZ1)/(Z02-Z01)
        V=VZ2-(Z02-Z)*(VZ2-VZ1)/(Z02-Z01)
49    CONTINUE
        XX=Z/XL
        XR=ZR/XL
        IF((Z.GT..234).OR.(Z.LT..058)) GO TO 55
        IF(Z.LT..1001) GO TO 52
        IF(Z.LT..140) GO TO 51
C FOR MAJOR DOWNDRAFT WE HAVE W FOR ZD.GE.Z.GT.ZR
50    W=-P1*A*SIN(3.1415927*(XX-XR)/Q1)
        RETURN
C FOR MAJOR UPDRAFT WE HAVE W FOR ZR.GE.Z.GE.ZR-L
51    WN=(A*(XR-XX)/Q0)*((2*Q0+1)*((XR-XX)**2-1)-(3*Q0**2-1)*(XR-XX+1))
        WD=((2*Q0+1)*(Q0**2-1)-(3*Q0**2-1)*(Q0-1))
        W=WN/WD
        RETURN
C FOR MINOR UPDRAFT AND MINOR DOWNDRAFT WE HAVE W FOR Z BOUNDED BY:
C MINOR UPDRAFT, ZR-(1+Q2)*L.GT.Z.GE.ZR-(1+Q2)*L
C MINOR DOWNDRAFT, ZR-L.GT.Z.GE.ZR-(1+Q2)*L
52    W=-P2*A*SIN(3.1415927*(XR-1-XX)/Q2)
        RETURN
C Z OUT OF RANGE
55    W=0
        RETURN
        END

```

```
SUBROUTINE WIND 5(X,Y,Z,U,V,W)
C THIS PROFILE IS FOR NIGHTTIME STABLE LAYER BOUNDARY (SEVERE)
C PROFILE FOR NO VARIATION OF WIND DIRECTION WITH ALTITUDE.
C EXPECTS DISTANCE IN KILOMETERS , GIVES UZ IN METERS/SECOND.
C UZ AND Z0 ARE TABLE VALUES FOR LINEAR INTERPOLATION
C U009 IS VELOCITY AT .0091 KM.
    DIMENSION UZ(12),Z0(12)
    DATA (UZ=3.952,5.954,10.060,12.164,16.630,15.398,13.447,12.626,
&11.754,11.600,11.446,11.446)
    DATA (Z0=.0091,.0228,.0457,.0914,.1371,.1828,.2286,.2743,.3200,
&.3657,.3962,.4572)
    U009=UZ(1)
    U=V=W=0.
    IF(Z.LE.0.0)RETURN
C FIND HEIGHT INTERVAL I
    DO 90 J=1,12
    K=J
    IF(Z.LT.Z0(J)) GO TO 95
90    CONTINUE
C MODEL FAILS FOR THIS Z.
    RETURN
95    I=K
    IF(I.GT.1) GO TO 5
4    U=U009*(Z/.0091)**.45
    RETURN
C DO LINEAR INTERPOLATION FOR I=2,12
5    UZ1=UZ(I)
    UZ2=UZ(I-1)
    Z01=Z0(I)
    Z02=Z0(I-1)
    U=UZ2-(Z02-Z)*(UZ2-UZ1)/(Z02-Z01)
    RETURN
    END
```

```

        SUBROUTINE WIND 6(X,Y,Z,U,V,W)
C ROUTINE TO COMPUTE A DOWNBURST WITH CENTER AT (XC,YC),
C SCALE HEIGHT H, AND WIND SCALE W0.
C THE FUNCTION, WHICH OBEYS CONTINUITY IS
C VR=W0*(A/H)**2*Z*EXP(-Z**2/H**2)*(1-EXP(-(R/A)**2)/R
C W=-W0*(1-EXP(-(Z/H)**2)*EXP(-(R/A)**2)
C LET A BE .5 KM, H BE .1 KM, W0 BE 6 M/S
        W0=6.
        A=.5
        XC=0.5
        YC=0.5
        H=.1
        DX=X-XC
        DY=Y-YC
        R2=DX**2+DY**2
        IF(R2.EQ.0) 10,20
10      ER=1.
        R=0.
        GO TO 30
20      ER=EXP(-R2/A**2)
        R=SQRT(R2)
30      CONTINUE
        EZ=EXP(-(Z/H)**2)
        IF(R.EQ.0) 40,50
40      U=V=0
        GO TO 60
50      RFACT=(1.-ER)/R
        VR=W0*(A/H)**2*Z*EZ*RFACT
        U=VR*DX/R
        V=VR*DY/R
60      CONTINUE
        W=-W0*(1.-EZ)*ER
        RETURN
        END

```